water

Article

Site-Specific Evaluation of Canopy Resistance Models for Estimating Evapotranspiration over a Drip-Irrigated Potato Crop in Southern Chile under Water-Limited Conditions

Rafael López-Olivari [1,*], Sigfredo Fuentes [2], Carlos Poblete-Echeverría [3], Valeria Quintulen-Ancapi [4] and Leovijildo Medina [4]

1 Instituto de Investigaciones Agropecuarias, INIA Carillanca, km 10 Camino Cajón-Vilcún s/n, Temuco Casilla Postal 929, Chile
2 Digital Agriculture, Food and Wine Sciences Group, School of Agriculture and Food, Faculty of Veterinary and Agricultural Sciences, The University of Melbourne, Parkville VIC 3010, Australia; sigfredo.fuentes@unimelb.edu.au
3 South African Grape and Wine Research Institute (SAGWRI), Department of Viticulture and Oenology, Faculty of AgriSciences, Stellenbosch University, Private Bag X1, Matieland 7602, South Africa; cpe@sun.ac.za
4 Departamento de Ciencias Agropecuarias y Acuícolas, Facultad de Recursos Naturales, Universidad Católica de Temuco, Temuco P.O. Box 15-D, Chile; vquintulen2015@alu.uct.cl (V.Q.-A.); lmedina@proyectos.uct.cl (L.M.)
* Correspondence: rafael.lopez@inia.cl

Abstract: The evapotranspiration (ET) process is an essential component in many agricultural water management systems, and its estimation is even more determinant when crops are grown under water-limited environments. The traditional canopy resistance (r_c) approaches were evaluated to simulate potato evapotranspiration (ET_{cp}) using the original Penman–Monteith equation under different irrigation levels. A field study was carried out on a drip-irrigated potato crop (var. Puyehue INIA) located in the Research Center Carillanca (INIA), La Araucanía Region, Chile (38°41′ S, 72°24′ W, 188 m above sea level) during the 2018/2019 and 2019/2020 growing seasons. The different irrigation levels were full irrigation (IL_1), 75% of IL_1 (IL_2), and 60% of IL_1 (IL_3). The soil water content, morphological, physiological, meteorological, and micrometeorological variables were measured to calculate the different r_c approaches and estimate ET for both growing evaluated seasons. The final values of estimated ET_{cp} were compared to the soil water balance method (ET_{cpWB}). The use of amphistomatous (LA) and hypostomatous (LH) r_c approaches are the best alternative to estimate the ET_{cp} on potato crops. The best estimation of ET was found for ET_{cpLA} with an overestimation of 0.6% for IL_1, 7.0% for IL_2, and 13.0% for IL_3, while for ET_{cpLH} with underestimations of 12.0, 11.0 and 31.0% for IL_1, IL_2, and IL_3, respectively. The lowest average values of root mean square error (RMSE), mean absolute error (MAE), and index of agreement (d) were observed for ET_{cpLA} in both IL_1 and IL_2 conditions, with values of 4.4 and 3.2 mm, 3.2 and 2.5 mm, and 0.82 and 0.87, respectively. More investigation is necessary on the plasticity of the morphological features of potato leaves and canopy geometry, as the stomatal water vapor flowing on the canopy surface could be affected, which is a key factor in the canopy resistance model for accurate ET estimation under soil-water-limited conditions.

Keywords: deficit irrigation; stomatal resistance; evapotranspiration; phenology

Citation: López-Olivari, R.; Fuentes, S.; Poblete-Echeverría, C.; Quintulen-Ancapi, V.; Medina, L. Site-Specific Evaluation of Canopy Resistance Models for Estimating Evapotranspiration over a Drip-Irrigated Potato Crop in Southern Chile under Water-Limited Conditions. *Water* **2022**, *14*, 2041. https://doi.org/10.3390/w14132041

Received: 26 May 2022
Accepted: 18 June 2022
Published: 25 June 2022

1. Introduction

Potato (*Solanum tuberosum* L.) is the world's fifth-most significant food crop (370 million tons) after rice, wheat, maize, and sugar cane, with a cultivated surface of 17.3 million hectares worldwide [1]. FAO has also highlighted it as a strategic and critical crop for food security due to its extraordinary environmental plasticity and its relative simplicity for cultivation and high nutritional value [2]. These characteristics have led to steady increases in potato consumption within developing countries [3]. Potato is the second staple food in Chile after wheat, reaching an average yield of 29 t ha^{-1} [4]. Of the total potato area cultivated in Chile, 57% is in the south between La Araucanía and Los Lagos regions [4] (between 38.0° S and 41.5° S latitude).

Climate change has affected, among other factors, the distribution and frequency of precipitation, mainly in the temperate and Mediterranean climatic zones [5,6]. In temperate climates, such as in La Araucanía Region and much of Southern Chile, droughts are more intermittent and unpredictable. Therefore, water availability can be the main limiting factor for uniform potato production throughout the growing season.

Researchers have considered deficit irrigation (DI) as the most appropriate approach for irrigation scheduling to manage water scarcity to increase water use efficiency (WUE) and harden the plants physiologically based on chemical signaling (mainly abscisic acid -ABA in leaves and stomata) [7]. For potato, some adaptations of the DI technique were tested in recent years, such as sustainable deficit irrigation (SDI), regulated deficit irrigation (RDI) and partial root-zone drying irrigation (PRD). In SDI, a uniform application of water restriction is supplied throughout the crop phenological development [8]. RDI is generally defined as an irrigation practice, where a crop is irrigated with an amount of water, which is below the full requirement for optimal crop growth [9]. At the same time, PRD is an alternated irrigation within the root zone by watering one furrow and keeping the adjacent one dry until the next watering cycle is applied. The watering regime is changed [10]. These DI techniques have been used as potential alternatives for irrigation scheduling due to their positive effects, such as increased WUE with minimal effects on yield, and improved sensory quality traits [9–16]. The implementation of DI practices also can reduce by nearly two-fold the leaf area, reaching leaf area index values (LAI) lower than three at harvest, compared to full irrigation regimes [7,13]. Furthermore, Carli et al. [17] observed that the canopy cover was strongly affected by water limitations compared to full irrigation reaching values lower than 70% without a significant effect on potato tubers' yield.

Potato plants have a relatively low sensitive response to water deficit in water-limited environments, making them an excellent candidate for evaluating the performance of estimative techniques for plant water status and water use, such as canopy resistance models. Researchers have shown that soil-imposed water stress would exert a significant impact on canopy resistance and evapotranspiration (ET). However, the accurate quantification of the effect of the soil water status on canopy resistance to water transfer and ET is still a big challenge [18–25]. Thus, the evapotranspiration (ET) process is an essential component of water and energy cycles on the Earth and for many agricultural water management studies. Accurate quantification of ET is imperative and key for optimizing the irrigation water use under scarce water resources [26,27].

In general, irrigation scheduling in potatoes is based on the quantification of the actual evapotranspiration (ET_a) using the traditional reference evapotranspiration (ET_o) and crop coefficients (K_c) [28]. The most significant uncertainty within this approach is that many of the K_c values reported in the literature are determined for specific situations and often not adapted to all conditions [29,30]. The latter problem is particularly significant since the ratios of ET to ET_o are highly dependent on the non-linear interactions among atmospheric conditions, soil type, cultivars, and irrigation management practices [31]. The Penman–Monteith model (PM) has been the most widely used method to estimate ET under drying conditions worldwide [19,25,28,32]. However, for increasing ET estimation accuracy, the parameterization of empirically and semi-empirical canopy resistances is critical since local conditions should be considered.

Currently, the classical canopy resistance (r_c) models are used in sparse or dense canopies, using well-watered conditions only [25,32–42]. All these r_c models were evaluated by Li et al. [43] for sparse canopy crops (maize and grapevines) with LAI between 0 and 5.8 and under well-watered conditions; the best resistance model performance results were those proposed by Li et al. [44] (coupled resistance model; soil + plant), Irmak and Multiibwa [42] and Katerji and Perrier [34] (agreement estimation in the entire growing season) with r^2 values close to 0.70, 0.60 and 0.56, respectively. The evaluation of r_c and

ET models in potatoes under different available soil water conditions can bring better information for implementing appropriate irrigation management strategies to maximize water use for this crop. These models are crucial for evaluating other drought tolerance crops due to prolonged drought in the Mediterranean, tropical, and temperate climate conditions worldwide.

For proper use of the ET models under water-limited environments, it is necessary to accurately determine r_c under these conditions, in addition to further understanding how the variables and parameters of the r_c models are affected by diurnal meteorological factors and soil water stress conditions. Thus, the main objective of this study was to evaluate and compare the use of traditional r_c models with the original Penman–Monteith equation considering the main phenological stages of a potato crop and under different irrigation levels in a temperate climate.

2. Materials and Methods

2.1. Site Description

The experiments were carried out at the Regional Research Center Carillanca from the Instituto de Investigaciones Agropecuarias (INIA), La Araucanía Region, Chile (38°41′ S, 72°24′ W, 188 m above sea level). A drip-irrigated potato crop (*Solanum tuberosum* L.) var. Puyehue-INIA (Chilean cultivar; [45] was used in a total experimental surface of 900 m^2 on a flat ground field (300 m^2 for each evaluated irrigation strategy) during the 2018/2019 and 2019/2020 growing seasons. The plantation density was 0.25 m inter-row × 0.75 m between-row, starting mid-December (Day of year—DOY 344) and November (DOY 315) for the first and second seasons. The effective rooting depth ($P_{effective}$) was down to 30 cm (with over 80% of active roots) for the well-watered condition determined through a soil pit at the end of each evaluated season. The experimental site presents a typical temperate climate, and it has been described in detail by López-Olivari and Ortega-Klose [46]. The soil is classified as Temuco series (Andisol, family Typic Hapludands) with a silty loam texture [47]. The values of organic matter content, bulk density, field capacity, and wilting point were 13.4%, 0.79 g cm^{-3}, 0.52, and 0.27 m^3 m^{-3}, respectively. For the 2018/2019 season, fertilization was based on a total dose of 210 kg ha^{-1} of P (at planting), 120 kg ha^{-1} of K and 240 kg ha^{-1} of N (both 60% at planting and 40% before hilling the potatoes). During the 2019/2020 season, fertilization was based on a total dose of 350 kg ha^{-1} of P (at planting), 160 kg ha^{-1} of K, and 120 kg ha^{-1} of N (both 60% at planting and 40% before hilling the potatoes). Preventive management for pests and diseases of potato plants was carried out during both seasons by applying a broad-spectrum insecticide (chemical group: pyrethroid + neonicotinoid) and fungicide (chemical group: carbamates + pyridinyl-methyl-benzamide) specific for the potato crop. Thus, the insecticide and fungicide were applied from 2 to 3 and 3 to 4 times along the evaluated seasons. Finally, the weed control was performed using a pre-emergence herbicide (chemical group: metribuzin) and a hand weeding control (every 10–15 days) throughout the season.

2.2. Deficit Irrigation Treatments and Irrigation Management

The potato plants for this trial were subjected to three different irrigation strategies: IL_1 (full irrigation), IL_2 (75% irrigation application of IL_1) and IL_3 (60% irrigation application of IL_1). The amount of irrigation applied for each irrigation strategy (sub-plot of 300 m^2) was defined using the dripper flow rate per plant (Netafim Ltd., Tel Aviv, Israel) manually inserted into the drip irrigation lines. For IL_1 and IL_2, one pressure-compensating button dripper per plant was used with a discharge of 4.0 and 3.0 L h^{-1}, and both separated at 0.25 m, respectively. In the case of IL_3 two pressure-compensating button drippers per plant were used with a discharge of 1.2 L h^{-1} each (total 2.4 L h^{-1}) separated at 0.25 m. The irrigation for IL_1 was calculated based on the concept of the total available soil water (TAW; mm), soil water depletion fraction (p), and readily available soil water (RAW; mm) [28]. A p equal to 0.35 was used [28], and this factor was maintained for the whole growing season [46,48–50]. The irrigation events were performed when 35% of TAW was depleted from the effective rooting zone. The soil moisture of each irrigation level was monitored using Frequency Domain Reflectometry (FDR; ECH2O GS-1 and GS-3, METER Group, Inc., Pullman, WA, USA). The irrigation frequency was defined using the reading of the FDR sensor from full irrigation conditions (IL_1). The irrigation time was determined by incorporating the readily available water (RAW) concept, the discharge of the drippers, and irrigation efficiency. The effective daily rainfall (R_{eff}) was determined using the expression

$$R_{eff} = (\text{pluviometric precipitation} - 10) \times 0.75, \quad (1)$$

These values were incorporated as the water contribution for irrigation scheduling [46].

2.3. Soil Moisture and Plant Measurements

2.3.1. Soil Moisture Monitoring

Five FDR probes were installed in a representative area for continuous measurements of volumetric soil moisture along the two growing seasons considered (after hilling the potato) for each evaluated irrigation strategy. For IL_1, an FDR ECH2O GS-3 probe was installed at a depth of 10 cm and four FDR ECH2O GS-1 probes at depths of 20, 30, 40, and 50 cm, respectively. For IL_2 and IL_3, five FDR ECH2O GS-1 probes were installed at depths of 10, 20, 30, 40, and 50 cm. Each set of FDR probes was used to measure the variation of soil moisture in the effective rooting zone. All readings were recorded in 15 min intervals using three different dataloggers (Em50 solar datalogger, METER Group, Inc., Pullman, WA, USA). Before installing the sensors on the soil of varying irrigation strategies, all of the sensors were calibrated externally on an undisturbed soil cube removed from the experimental site following the method proposed by López-Olivari and Ortega-Klose [46]. Furthermore, the volumetric soil water content at the soil surface layer (0–10 cm depth) was measured next to the soil heat flux plates located in-row and between-row using another set of two FDR TEROS 10 probes, where the data were recorded in 15 min intervals in a datalogger (ZL-6 solar datalogger, METER Group, Inc., Pullman, WA, USA) located in each evaluated irrigation conditions (Figure 1).

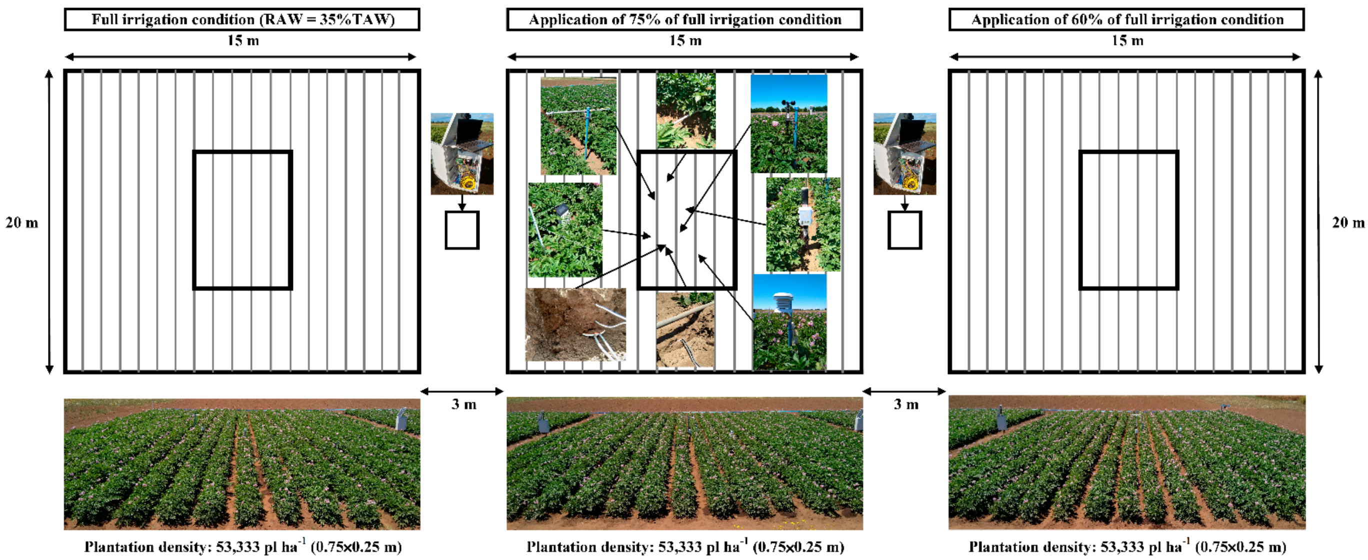

Figure 1. The general layout of the set instruments implemented in each evaluated irrigation levels conditions. At the central point of each irrigation level, the following instruments were installed: net radiometers, soil heat plates, and soil temperature probes, volumetric soil moisture sensors (for soil heat plates and soil water balance determinations), hygrometers, and anemometers. RAW and TAW are readily available soil water and total available soil water, and 35% is the p value according to Allen et al. [28].

2.3.2. Stomatal Conductance

Daytime measurements of stomatal resistance ($r_{st} = 1/g_{st}$) were performed in five plants for each evaluated irrigation strategy (n = 10) using a steady-state porometer (SC-1 leaf porometer, METER Group, Inc., Pullman, WA, USA). The r_{st} measurements were performed in two non-damaged, fully expanded, sunlit, and mature leaves located in the upper canopy layer of each plant every two hours from 08:00 to 20:00 h. The frequency of measurements was determined before each irrigation event during the growing season.

2.3.3. Leaf Area Index (LAI) and Phenology

The leaf area index (LAI) was obtained by extracting weekly two representative plants per irrigation strategy throughout the growing season. The leaves of each plant were photographed on a known surface. The total leaf area per plant was determined using the free Image J software [51] and the methodology proposed by Rolando et al. [52]. The crop height (h_c) was measured weekly with a measuring tape from five marked plants growing on the field during the whole phenological period.

The phenological stages were evaluated based on the Biologische Bundesanstalt, Bundessortenamt, and Chemical Industry (BBCH) scale [53], considering the following as the main stages: establishment (E), leaf development (LD), inflorescence emergence (IE), flowering (F), fruit development (DF), ripening of fruit and seed (RF), senescence (S) and harvest (H).

2.4. Micrometeorological and Meteorological Measurements

All meteorological instrumentation was installed after hilling the potato (fraction cover close to 15%) in the central area from each irrigation treatment plot (5–6 m from edges) (Figure 1). The same set of micrometeorological equipment was installed in each evaluated irrigation strategy, which consisted of (i) wind speed (u) by three-cup young wind sentry anemometer (Model 03101, RM Young Co., Traverse City, MI, USA); (ii) air temperature (T_a) and relative humidity (RH) measured by an Onset probe (model HOBO Pro v2) installed near the potato canopy. The sensors of u, T_a and RH were moved upward as the potato plants were growing to maintain a height difference between the sensor and the top of the potato plant canopy of 0.2 m. (iii) Net radiation (R_n) was measured by two net radiometers (NR-Lite2, Kipp&Zonen, Inc., Delft, the Netherlands) located above the plant row at 1.0 m from the soil surface and another below of the canopy. (iv) Soil heat flux (G) was estimated using two heat flux plates of constant thermal conductivity (HFP01, Hukseflux, Delft, the Netherlands), one located between rows and the second one in the row for each irrigation level implemented. This arrangement accounted for the row shade effect during the daytime [54]. The soil heat flux plates were installed at a depth of 0.08 m. (v) Finally, the soil temperature (T_s) was measured by one averaging thermocouple probe (TCAV, Campbell Sci., Logan, UT, USA) installed above each flux plate at 0.02 and 0.06 m depths. The final value of soil heat flux (G) was determined by adding the measured flux at 0.08 m and the heat stored (S) in the layer above each heat flux plate [55]. The S values can be computed as follows:

$$S = (\rho_b C_d + \theta_v \rho_w C_w)\frac{\Delta T_{soil}}{\Delta t}d, \tag{2}$$

where ρ_b is the soil bulk density (790 kg m^{-3}); ρ_w is the density of water (1000 kg m^{-3}); C_d is the specific heat capacity of dry allophane soil (J kg^{-1} K^{-1}); θ_v is the volumetric soil moisture (m^3 m^{-3}); C_w is the specific heat capacity of the soil water (4186 J kg^{-1} K^{-1}); ΔT_{soil} is the change in soil temperature (K); Δt is the time intervals (s); and d is the soil thinkness (m). Values between 959 and 1340 J kg^{-1} K^{-1} for C_d are reasonable for most allophane soils [56–58]. An average value of C_d equal to 1150 J kg^{-1} K^{-1} was used in this study.

Finally, the average values of soil heat flux (G) were determined according to

$$G = G_{IR} f_c + G_{BR}(1 - f_c), \tag{3}$$

where f_c is a fraction of cover (dimensionless) calculated using the averaged canopy width and distance between rows, and G_{IR} and G_{BR} are G values (W m^{-2}) in rows and between rows of the potato, respectively.

All the measurements for R_n, G, u, T_s were recorded on two electronic dataloggers (CR1000, Campbell Scientific Inc., Logan, UT, USA) for each irrigation level at 15 min intervals. Additionally, a Campbell Scientific Automatic Weather Station (AWS) measuring solar radiation (R_s), precipitation (P_p), wind speed (w_{2m}) and direction at 2 m (w_{2m}), T_{a_AWS}, and RH_{AWS} sensors were installed under the FAO56 reference condition near the experimental site (linear distance of 450 m).

2.5. Statistical Analysis

For the potato ET comparisons included ET_{cp}/ET_{cpWB} (r_{eo}) ratio, the root mean square error (RMSE), mean absolute error (MAE), index of agreement (I_a) and t-statistic [59–61] were used. Additionally, the z-test was determined to check whether the slope value of r_{eo} was significantly different from 1.0 at the 95% confidence level. Analysis of variance was performed on stomatal conductance and resistance variables. In those cases, the post-hoc mean comparison was made using Tukey's HSD test with a p value of 0.05.

3. Biophysical Algorithms Implemented

3.1. Canopy Resistance Approaches (r_c)

The r_c was determined using a daytime frequency from 8:00 to 18:00, where the input variables for all models were considered between 14:00 and 16:00 h (maximum water demand from the atmosphere). The r_c model under deficit irrigation in potato was evaluated using three approaches: (i) Szeicz and Long [62] (SL), (ii) Allen et al. [28] (AL), and (iii) Lhomme et al. [63] (L). For this study, all r_c values were mainly calculated for the period of maximum water demand from the atmosphere during both seasons.

3.1.1. SL Approach

In this empirical model, the r_c is calculated using a leaf stomatal resistance (r_{st}, s m^{-1}) and the effective LAI (LAI_{eff}, m^2 m^{-2}) is measured throughout the phenological stages, which is the portion of the canopy from which the bulk of transpiration occurs. Thus, the determination of the empirical function r_{SL}^c (s m^{-1}) is calculated according to the following equation [62,64]:

$$r_{SL}^c = \begin{cases} r_{st}/LAI \quad , & for\ LAI \leq 0.5LAI_{thr} \\ r_{st}/LAI_{eff}, & for\ LAI > 0.5LAI_{thr} \end{cases}, \tag{4}$$

where LAI_{thr} is the threshold LAI frequently taken as the maximum LAI of the plant (average value for both seasons of 3.7; 3.1 and 2.7 m^2 m^{-2} for IL_1, IL_2, and IL_3, respectively). Thus, LAI_{thr} depended on the irrigation water levels implemented in this study.

3.1.2. AL Approach

In this model, the r_c is calculated using the average stomatal resistance (r_{st}) of an individual leaf divided by the active (sunlit) leaf area index (LAI). The LAI represents the leaf area (upper side only) per unit area of soil below it (0.5LAI), where the effective LAI is the index of the leaf area that actively contributes to the surface heat and vapor transfer [28].

$$r_{AL}^c = \frac{r_{st}}{LAI_{eff}} \text{ where } LAI_{eff} = 0.5LAI, \tag{5}$$

3.1.3. L Approach

In this model, the r_c is calculated using a leaf stomatal resistance r_{st} (one side), where it should be divided by the transpiring surface, expressed per unit area of land surface: 2LAI for amphistomatous leaves (LA model) and only LAI for hypostomatous leaves (LH model) proposed by Lhomme et al. [63]. For convenience, they introduce the parameter n

(n = 1 for amphistomatous leaves and n = 2 for hypostomatous leaves), which allows the canopy resistance to be written as

$$r_L^c = \frac{nr_{st}}{2LAI}, \tag{6}$$

However, the literature has reported that potato plants could have hypostomatous leaves [65,66] or amphistomatous leaves [67], so both approaches were considered.

3.2. Evaluation of the r_c Models through ET Calculation

Each of the r_c modeling approaches evaluated during the 2018/2019 and 2019/2020 seasons were incorporated into the Penman–Monteith equation to estimate the daily potato evapotranspiration (ET_{cp}, mm day^{-1}) according to the following expression [68]:

$$ET_{cp} = \frac{1}{\lambda}\frac{\Delta(R_n - G) + K_{time}c_p\rho_a D_{pv}r_a^{-1}}{\Delta + \gamma\left(1 + r_c r_a^{-1}\right)}, \tag{7}$$

where Δ is the slope of the saturation vapor pressure curve at the mean temperature (kPa °C^{-1}), R_n is the net radiation (MJ m^{-2} day^{-1}), G is the soil heat flux (MJ m^{-2} day^{-1}), c_p is the specific heat of the air at constant pressure (MJ Kg^{-1} °C^{-1}), ρ_a is the air density (Kg m^{-3}), D_{pv} is the vapor pressure deficit of air (kPa), γ is the psychrometric constant (kPa °C^{-1}), r_c is the bulk canopy resistance (s m^{-1}), r_a is the aerodynamic resistance (s m^{-1}), λ is the latent heat of vaporization of water (MJ kg^{-1}), and K_{time} is the unit conversion equal to 86,400 s day^{-1}.

The mathematical expression used for the aerodynamic resistance, which describes the resistance of vapor flow moving from the evaporating surface into the air above the canopy, is as follows:

$$r_a = \frac{ln\left(\frac{(z-d)}{z_0}\right) ln\left(\frac{(z-d)}{(h_c-d)}\right)}{k^2 u(z)}, \tag{8}$$

where z is the reference height (m), d is the zero-plane displacement (m), h_c is the crop height (m), z_0 is the roughness length of the crop relative to momentum transfer (m), k is the Karman's constant (0.41), and $u(z)$ is the wind speed at height z (m s^{-1}). For the potato crop, the specific values of z_0 can be determined as 0.041h_c and d as 0.78h_c [69].

The estimated ET_{cp} was compared to the measured ET_{cpWB} using the soil water balance approach of the root zone proposed by Allen et al. [28] for the different implemented irrigation conditions that were evaluated using the following expression:

$$ET_{cpWP,i} = (P - RO)_i + I_i + CR_i - DP_i - (D_{r,i} - D_{r,i-1}), \tag{9}$$

where $ET_{cpWP,i}$ is the crop evapotranspiration on day i (mm), P_i is the precipitation on day i (mm), RO_i runoff from the soil surface on day i (mm), I_i is the net irrigation depth on day i that infiltrates the soil (mm), CR_i is the capillary rise from the groundwater table on day i (mm), DP_i water loss out of the root zone by deep percolation on day i (mm), $D_{r,i}$ is the water depletion in the root zone at the end of day i (mm), $D_{r,i-1}$ is the water content in the root zone at the end of the previous day, $i - 1$ (mm). The term RO_i for the periods with heavy rainfall was measured indirectly by assuming that in such conditions, crop evapotranspiration (ET) is equal to the reference evapotranspiration (ET_o) according to Vachaud et al. [70] and Franco et al. [71]. However, RO_i for drip irrigation was assumed to be zero [72,73], but in the possible cases that the irrigation water amounts exceeded the cumulative soil water depletion at the 10 cm soil layer was treated as RO_i outside of the potato ridge. The CR_i was presumed to be zero because there was no evidence of a water table of at least 1 m in soil depth. On the other hand, the total amount of water under the effective rooting zone was considered to be lost by deep percolation (DP_i) according to data obtained from volumetric soil moisture sensors installed in the field. Finally, the final values of ET measured and estimated were summed and compared between irrigation events during both evaluated seasons.

4. Results and Discussion

4.1. Meteorological Measurements and Soil Moisture Conditions

The daily variation of rainfall (R), reference evapotranspiration (ET_o), air temperature (T_a), and vapor pressure deficit (VPD) during the 2018/2019 and 2019/2020 seasons are shown in Figure 2. There was a total cumulative rainfall (TCR) from the plantation to 15 days before harvest of 97.2 and 88.3 mm for the 2018/2019 and 2019/2020 seasons, respectively. Thus, the rainfall for the 2018/2019 season was mainly concentrated during the first days of December (DOY 344 to 348; plantation) and March (DOY 60 to 66; finishing development of fruits), while for the 2019/2020 season, it was during the first days of January (DOY 5 to 8; >50% of flower opening) and the first days of February (DOY 32 to 48; development of fruits; Figures 2 and 3). Furthermore, the maximum value of ET_o corresponded to 6.6 mm day^{-1} observed during a critical phenological period (DOY 45; flowering stage) for the first season. For the second season, a maximum value of 5.6 mm day^{-1} was observed during a non-critical phenological period (DOY 51; end of fruit development). For the 2018/2019 season, the maximum, minimum, and average values of T_a ranged from 12.2 to 37.9 °C, −1.4 to 15.2 °C, and 8.2 to 23.8 °C between emergence and 15 days before harvest (86 days). whereas for 2019/2020, the same T_a values ranged from 14.9 to 34.7 °C, −0.5 to 13.8 °C, and 11.6 to 20.1 °C between emergence and 15 days before harvest (91 days). Finally, during the 2018/2019 season, the tendency of VPD was similar to T_a and ET_o. The maximum, minimum, and average values varied from 0.2 to 4.9 kPa, 0.0 to 0.5 kPa, and 0.1 to 2.1 kPa between emergence and 15 days before harvest. For the 2019/2020 season, the maximum, minimum, and average values of VPD ranged from 0.8 to 5.1 kPa, 0.0 to 0.3 kPa, and 0.2 to 1.9 kPa between emergence and 15 days before harvest, respectively.

The variation of volumetric soil moisture and rainfall values for the different irrigation levels applied during the growth and development stages of the potato crop (IL_1, IL_2 and IL_3) for both seasons are shown in Figure 3. Two irrigation events were applied before hilling the potato and installing volumetric soil moisture sensors in both seasons. Thus, the total quantity of irrigation water supplied in those periods was 43 and 54 mm for the first and second seasons. A total of 13 irrigation events (including the two early irrigations before hilling the potato) were applied during the first season. Three effective rainfall (two before hilling the potato) were observed between emergence and 15 days before harvest, whereas 16 irrigation events (including the two early irrigations before hilling the potato) were supplied. Three effective rainfall events occurred between emergence and 15 days before harvest for the second season. During the first season, there was a period when the volumetric moisture depletion of the soil decreased slowly (DOY 47 to 54 and DOY 59 to 63). In this period, the potato crop there was in the phenological stage between the finishing of flowering and fruit development, and the main meteorological variables showed low average values ranging from 10.1 to 18.9 MJ m^{-2} d^{-1}, 11.6 to 18.3 °C, 0.24 to 0.58 kPa for the solar radiation (R_s), T_a, and VPD, respectively.

4.2. Stomatal Resistance Patterns under Irrigation Levels

The patterns of daytime stomatal resistance (r_{st}) and stomatal conductance (g_s) during the critical phenological stages of IE—DF for the three different irrigation levels are shown in Figure 4. Thus, there was a physiological response with a clear differentiation of the values r_{st} and g_s for the irrigation levels applied in this study, reaching a maximum difference between 14:00 and 18:00 on a potato crop [74]. Additionally, these g_s differentations were observed in potato leaves grown under a 12 h light and 12 h dark photoperiod at 350 ppm of CO_2 by Wheeler et al. [75]. In this case, the plants were grown at either 400 or 800 µmol m^{-2} s^{-1} photosynthetic photon flux (PPF). Furthermore, r_{st} and

g_s presented statistical differences between the 16:00 and 18:00 for the first season, while statistical differences were observed among 14:00 and 18:00 during the second season.

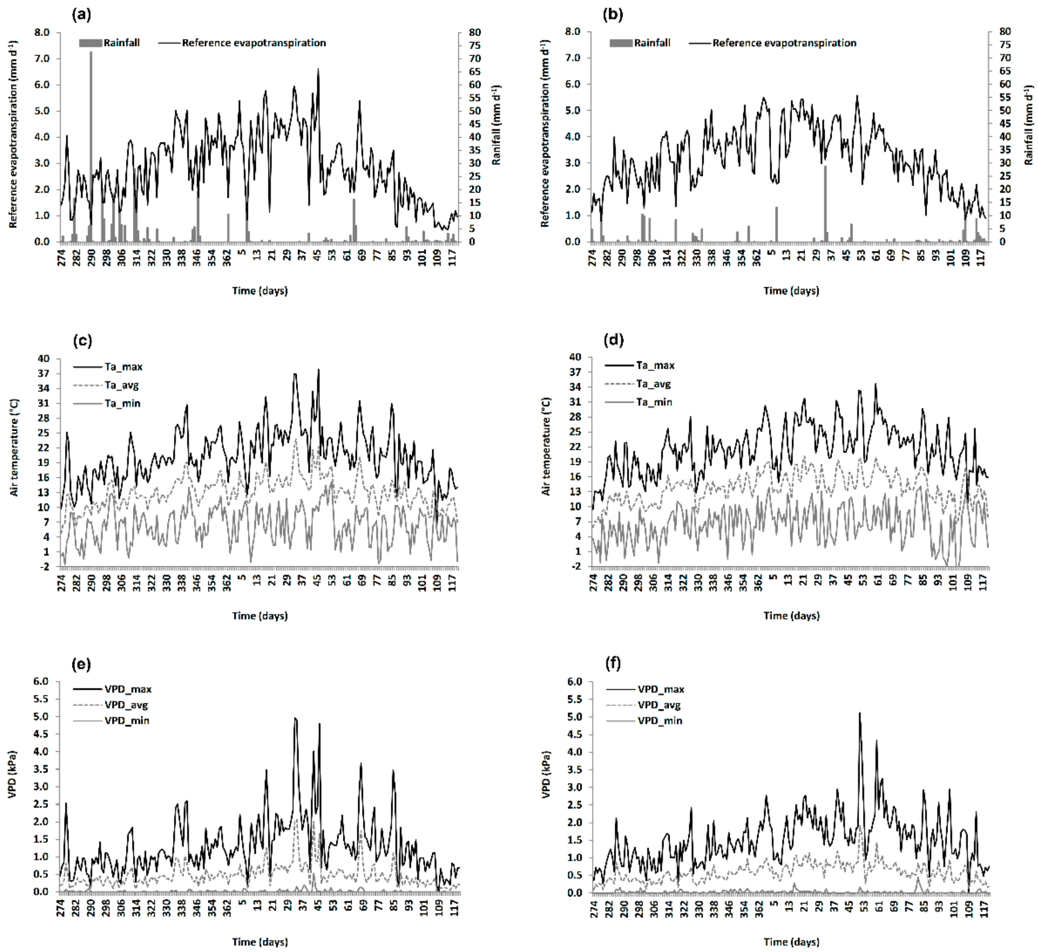

Figure 2. Daily variation of meteorological data registered by an automatic weather station (AWS) located close to study site for the 2018/2019 (**a**,**c**,**e**) and 2019/2020 (**b**,**d**,**f**) seasons. T_a is the air temperature, and VPD is the vapour pression deficit. The abbreviation max, avg and min are the measured variables' maximum, average, and minimum expression.

Although potato plants are susceptible to water stress and the decrease in available soil moisture, the plants presented a significant partial stomatal closure at the most stressed irrigation levels implemented. This response could vary due to the morphophysiological features of the different potato genotypes/cultivars [76]. Thus, Sun et al. [77] found that stomatal morphology in potato leaves has plasticity to soil moisture status and dynamics changes. They observed that under full irrigation (FI), the plants had the largest stomatal size, followed by the deficit irrigation (DI) condition, and partial root-zone drying (PRD) had the smallest. At the same time, the reverse was found for stomatal density (SD). In the same context, Sam et al. [78] observed differences in the anatomical characteristics of the leaf epidermis (on both sides of the leaf) in the cultivars that Desirée and Baraka subjected to three water-deficit conditions. For instance, the stomatal density for cv. Baraka increased in the adaxial surface with water stress, while it decreased for cv. Desirée.

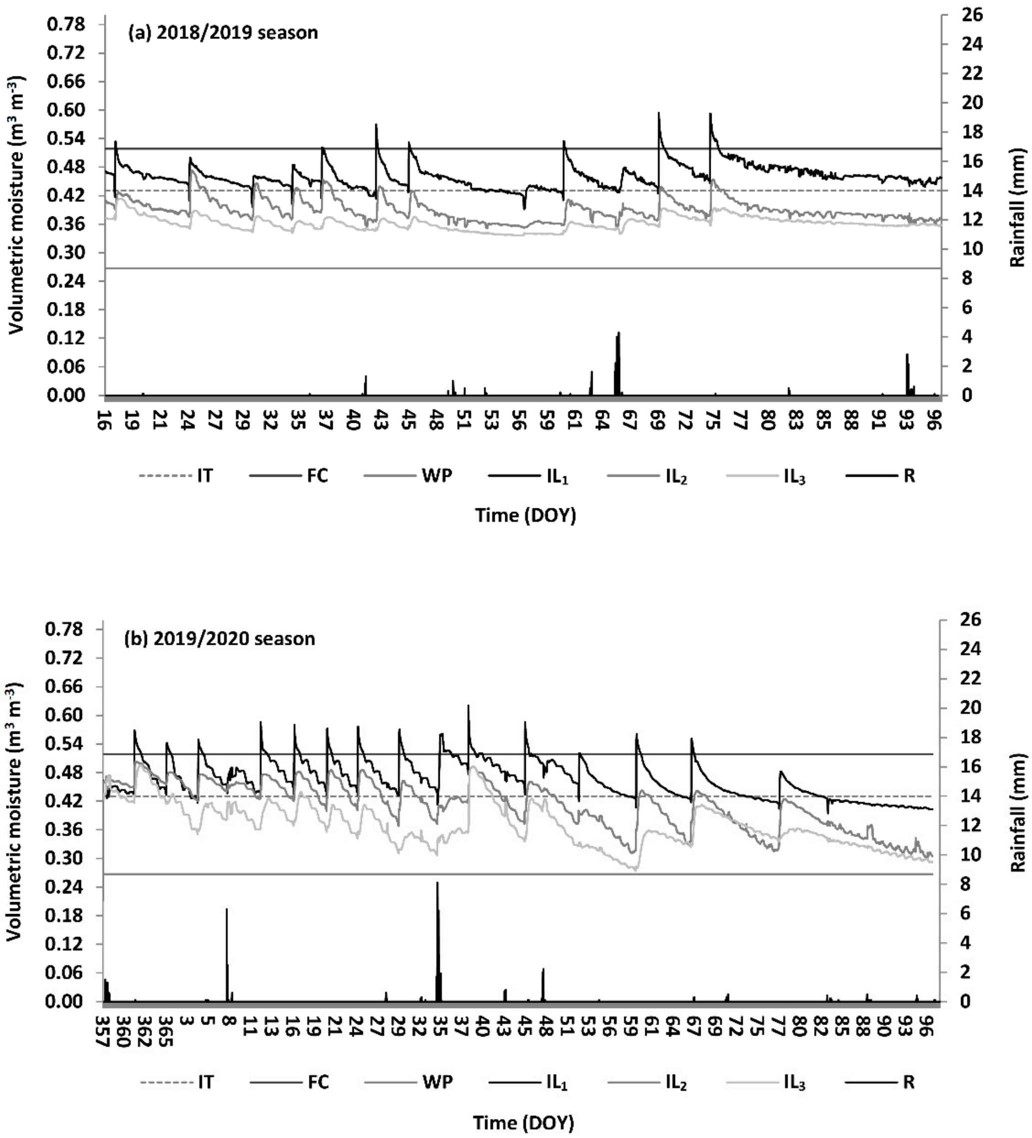

Figure 3. Variation of volumetric soil water content and rainfall measured values for the two evaluated seasons 2018/2019 (**a**) and 2019/2020 (**b**). The irrigation level (IL) was IL_1: Full irrigation, IL_2: 75% of IL_1, and IL_3: 60% of IL_1. IT, R, FC, and WP are irrigation threshold, rainfall, and soil water content at field capacity and permanent wilting point.

For the 2018/2019 season, the potato plant presented the lowest resistance to loss of water during midday time (12:00–14:00) with average r_{st} values of 43, 48, and 60 s m^{-1} for IL_1, IL_2, and IL_3, respectively, whereas average r_{st} values of 50, 54, and 65 s m^{-1} for IL_1, IL_2, and IL_3 were observed during the 2019/2020 season, respectively. In the same way, the highest water loss (>g_s) to the atmosphere was observed during the same hours when the lowest values of resistance to water loss occurred for both seasons. Thus, for the 2018/2019 season, maximum average g_s values of 0.922, 0.761, and 0.627 mol m^{-2} s^{-1} were observed during midday for IL_1, IL_2, and IL_3, respectively, whereas maximum average g_s values of 0.820, 0.760, and 0.664 mol m^{-2} s^{-1} were observed for the 2019/2020 season. In this context, similar average values of g_s were found on a potato crop cv. Folva ranged from 0.4 to 1.2 mol m^{-2} s^{-1} under both full irrigation and deficit irrigation (partial root-zone drying; PRD). The lower values were mainly obtained using the PRD strategy [7,13]. Furthermore, the average value of r_{st} between the LD–IE period increased 17.4 and 27.1% for IL_2 and IL_3 compared to IL_1, respectively.

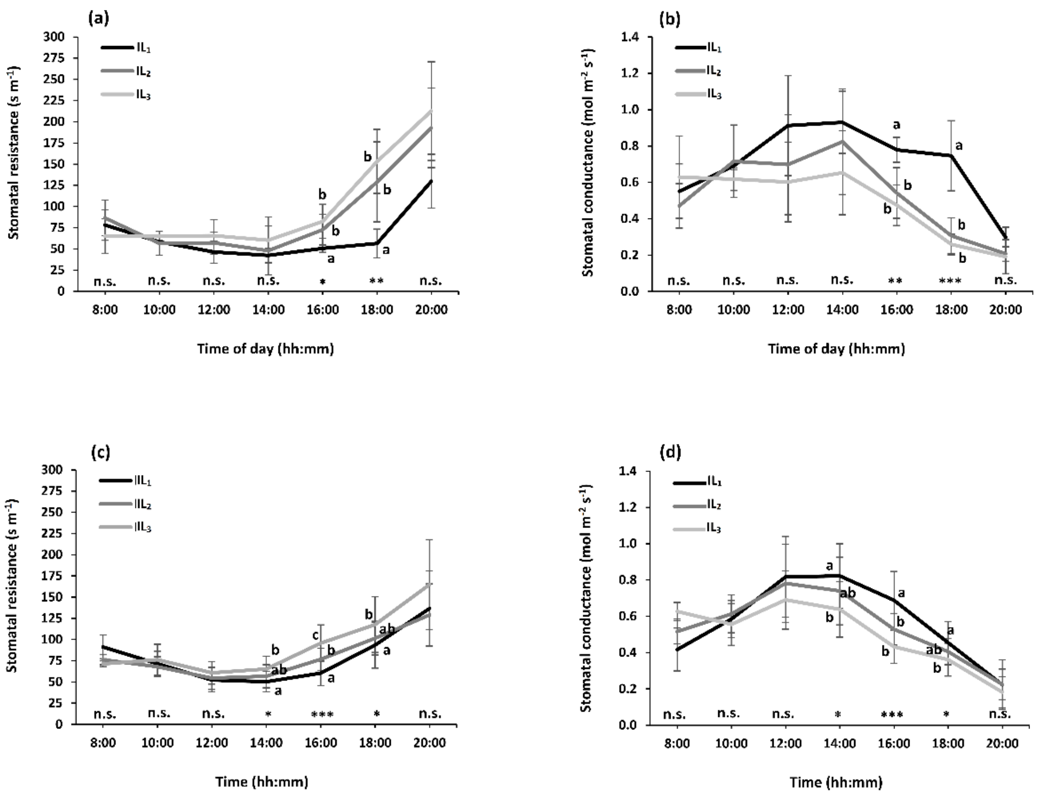

Figure 4. Representative average daytime values of stomatal resistance (r_{st}) and stomatal conductance (g_s) during the phenological stage inflorescence emergence–development of fruit (IF-DF) and maximum water atmospheric demand for the three different irrigation levels. DOY 35 to 45 for the 2018/2019 season (**a**,**b**) and DOY 3 to 20 for the 2019/2020 season (**c**,**d**). Error bars indicate ± SE (n = 5). AVOVA (n.s.: not significance when $p > 0.05$; * $p \leq 0.05$; ** $p \leq 0.01$; *** $p \leq 0.001$). According to the Tukey test HSD, the means in the same column with the same letter are not significantly different ($p \leq 0.05$). IL_1, IL_2, and IL_3 are full irrigation, application of 75% and 60% of IL_1, respectively.

For the range of phenological stages between IE–DF, the average r_{st} value increased 15.2 and 21.7% for IL_2 and IL_3 compared to IL_1, respectively. Moreover, there were increases of 19.2 and 46.1% in the average r_{st} value between the DF–RF period for IL_2 and IL_3 compared to IL_1, respectively. However, decreases of 13.0 and 27.4% were observed in the average r_{st} value between the DF–S period for IL_2 and IL_3 compared to IL_1, respectively (Table 1).

Table 1. Average values for both seasons of leaf area index (LAI), midday stomatal (r_{st}) and canopy (r_c) resistances for the empirical canopy resistance models (LA, LH, SL and AL) during the main potato phenological stages in the three irrigation levels (IL) conditions.

	Full Irrigation (IL_1)											
	LA			LH			SL			AL		
Phenological Stages	LAI (m^2 m^{-2})	r_{st} (s m^{-1})	r_c (s m^{-1})	LAI (m^2 m^{-2})	r_{st} (s m^{-1})	r_c (s m^{-1})	LAI_m (m^2 m^{-2})	r_{st} (s m^{-1})	r_c (s m^{-1})	LAI (m^2 m^{-2})	r_{st} (s m^{-1})	r_c (s m^{-1})
LD—IE	1.56	38.0	13.7	1.56	38.0	27.5	2.51	38.0	28.7	1.56	38.0	55.0
IE—DF	2.78	55.3	10.4	2.78	55.3	20.8	3.74	55.3	30.0	2.78	55.3	41.6
DF—RF	3.45	66.6	10.0	3.45	66.6	19.9	3.74	66.6	36.8	3.45	66.6	39.9
RF—FS	2.57	90.0	17.5	2.57	90.0	35.1	3.74	90.0	49.8	2.57	90.0	70.1

Table 1. *Cont.*

	Application of 75% of IL_1 (IL_2)											
	LA			LH			SL			AL		
Phenological Stages	LAI (m^2 m^{-2})	r_{st} (s m^{-1})	r_c (s m^{-1})	LAI (m^2 m^{-2})	r_{st} (s m^{-1})	r_c (s m^{-1})	LAI_m (m^2 m^{-2})	r_{st} (s m^{-1})	r_c (s m^{-1})	LAI (m^2 m^{-2})	r_{st} (s m^{-1})	r_c (s m^{-1})
LD—IE	1.26	44.6	18.7	1.26	44.6	37.4	1.26	44.6	37.4	1.26	44.6	74.9
IE—DF	2.44	63.7	13.3	2.44	63.7	26.6	3.15	63.7	40.3	2.44	63.7	53.3
DF—RF	2.98	79.4	13.5	2.98	79.4	27.0	3.15	79.4	51.2	2.98	79.4	54.0
RF—FS	2.19	101.7	23.9	2.19	101.7	47.7	3.15	101.7	65.2	2.19	101.7	95.4
	Application of 60% of IL_1 (IL_3)											
	LA			LH			SL			AL		
Phenological Stages	LAI (m^2 m^{-2})	r_{st} (s m^{-1})	r_c (s m^{-1})	LAI (m^2 m^{-2})	r_{st} (s m^{-1})	r_c (s m^{-1})	LAI_m (m^2 m^{-2})	r_{st} (s m^{-1})	r_c (s m^{-1})	LAI (m^2 m^{-2})	r_{st} (s m^{-1})	r_c (s m^{-1})
LD—IE	0.98	48.3	26.5	0.98	48.3	53.1	0.98	48.3	53.1	0.98	48.3	106.1
IE—DF	2.21	75.8	17.7	2.21	75.8	35.3	2.79	75.8	54.6	2.21	75.8	70.6
DF—RF	2.43	97.3	20.2	2.43	97.3	40.4	2.79	97.3	71.8	2.43	97.3	80.8
RF—FS	1.71	114.7	34.6	1.71	114.7	69.3	1.92	114.7	87.5	1.71	114.7	138.6

Note: LA and LH are the r_c models incorporating the concept of amphistomatous and hypostomatous leaves [63], respectively. SL is the r_c model proposed by Szeicz and Long [62]. AL is the more used r_c model proposed by Allen et al. [28]. LAIm is the average leaf area index according to Equation (4). LD, IE, DF, RF and FS are leaf development, inflorescence emergence, development of fruit, ripening of fruit and seed, and finishing of senescence, respectively.

4.3. Canopy Resistance Patterns and ET_{cp} Estimation

The averaged midday values of the different canopy resistance (r_c) approaches for the main phenological stages under three irrigation levels supplied during the 2018/2019 and 2019/2020 seasons are shown in Figure 5. A parabolic tendency of the estimated r_c approaches [21,79], with different magnitude, along the main phenological stages and for the supplied irrigation levels (IL_1, IL_2 and IL_3) were found in this study. The same pattern was obtained in other crops [80–84]. Thus, the average values of r_c observed were 15, 30, 43, and 60 s m^{-1} for the LA, LH, SL, and AL approaches in the full irrigation (IL_1) condition during the 2018/2019 season, respectively. During the 2019/2020 season, the average r_c values of 11, 22, 30, and 43 s m^{-1} were observed for the LA, LH, SL, and AL approaches in the full irrigation (IL_1) condition (Figure 5a,b). However, with the application of 75% of IL_1, similar averaged values of r_c were obtained for the LA, LH, SL, and AL approaches with 18, 35, 52, and 70 s m^{-1} for the first season and 17, 34, 45, and 68 s m^{-1} for the second season, respectively (Figure 5c,d). For the application of 60% of IL_1, averaged values of r_c equal to 26, 51, 75, and 102 s m^{-1} and 24, 48, 59, and 96 s m^{-1} for the LA, LH, SL, and AL approaches were obtained during the 2018/2019 and 2019/2020 season, respectively (Figure 5e,f).

Amer and Hatfield [21] observed average midday values of r_c in potato close to 21 (DOY from 318 to 350) and 13 s m^{-1} (DOY from 85 to 119) under well-irrigated conditions (when soil moisture was reduced to 50% of total available water, TAW). Similar values of r_c at the beginning of the growing season were observed using LA approach in both seasons. Nevertheless, Kjelgaard and Stockle [79] reported in potato seasonal average values of r_c equal to 40 s m^{-1} under well-irrigated conditions (furrow irrigation), presenting the higher values at the beginning and finishing of the season. Moreover, the AL approach showed higher r_c in all phenological stages and irrigation levels. Still, it was higher during the LD-IF and close to the RF-S compared to the other evaluated approaches, which could be due to the lower values of effective LAI (a concept that uses this approach) that actively contribute to the surface heat and vapor transfer [28] and leave senescence by the maturing canopy [21] (Table 1). Furthermore, the pattern of the r_c values for each evaluated approach were similar during the developing periods of IF-DF and DF-RF for all irrigation levels implemented.

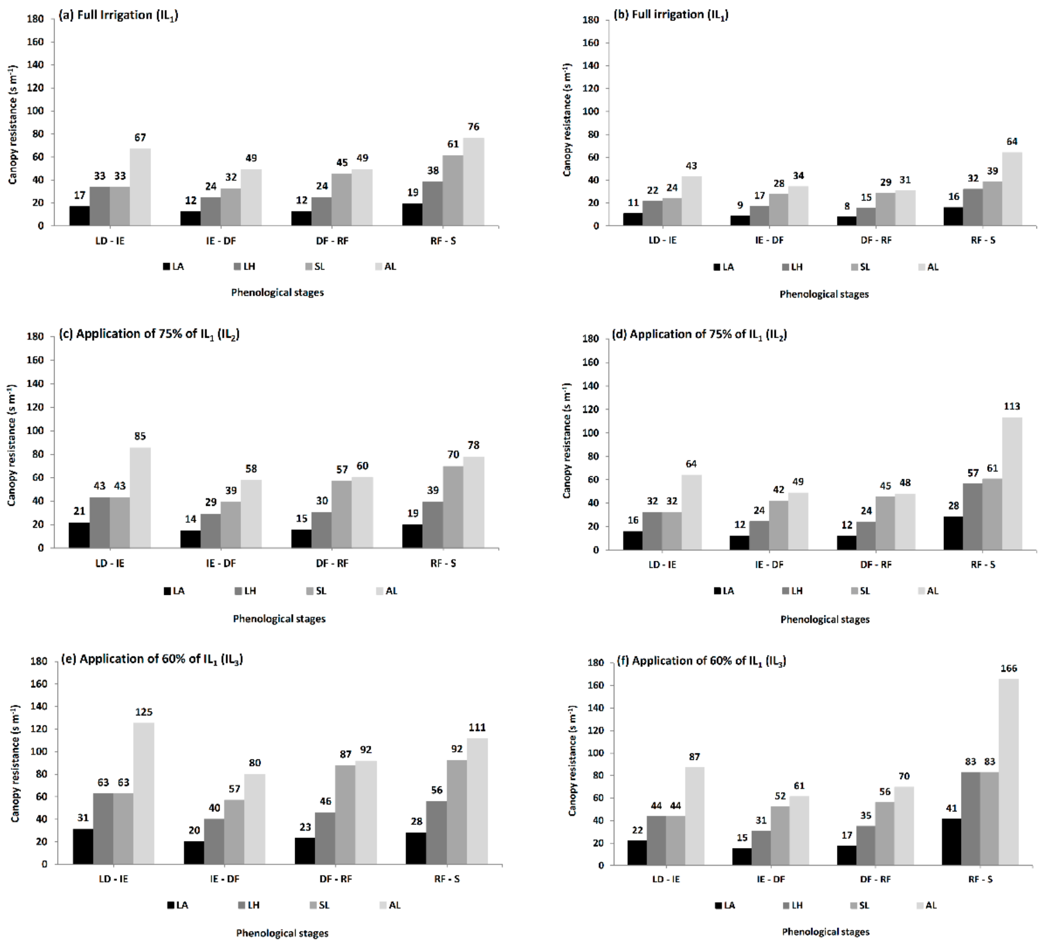

Figure 5. Midday average values (14:00–16:00) of canopy resistances (r_c) during the main potato phenological periods under different irrigation levels (IL) for 2018/2019 (**a**,**c**,**e**) and 2019/2020 (**b**,**d**,**f**) evaluated seasons. LA and LH [63], SL [62], and AL [28] are the empirical models of r_c used in this study. The potato phenological ranges LD-IE, IE-DF, DF-RF, and RF-S are leaf development–inflorescence emergence, inflorescence emergence–development of fruit, development of fruit–ipening of fruit and seed, and ripening of fruit and seed–finishing of senescence, respectively. These values were used to estimate crop potato evapotranspiration (ET_{cp}).

However, the tendency of LA and LH approaches for the different phenological stages and irrigation water levels implemented were more stable, reaching lower values in both seasons (Table 1). The latter could be related to the calculation of r_c for amphistomatous and hypostomatous leaves [63]. For this study, the leaves of the potato cultivar Puyehue INIA growing under temperate climate presented stomata on both sides of the leaf, where the abaxial surface presented a higher number of stomata in comparison to the adaxial surface for all implemented irrigation water levels conditions (data not shown). Thus, the calculation of r_c that considers the amphistomatous [67] and hypostomatous [65,66] potato leaves behaviors were determined in this study.

On the other hand, all the evaluated r_c approaches showed a plasticity response to the evident lack of available soil water in the effective rooting zone caused by the irrigation water deficit that affects potato plants' microclimate conditions. Thus, a decrease in the LAI and an increase in the r_c values were observed between irrigation water levels supplied throughout the evaluated growing seasons (Table 1). The charges of r_c observed as a consequence of the soil water available and the ambient conditions agreed with those found by Hatfield [85], Rana et al. [86], Kjelgaard and Stockle [79], and Amer and Hatfield [21]. In this study, the LA approach (amphistomatous leaves) presented similar values of r_c between IL_1 and IL_2 for the 2018/2019 and 2019/2020 seasons, where it could potentially be used under water-limited conditions up to 25%. Although in the literature, it is possible to find that r_c models that incorporate the dependence on soil moisture [32,39] have presented errors, especially during the sparse canopy stages in full irrigation crops [43,87].

Furthermore, it is necessary to incorporate detailed measurements of the anatomical characteristics of leaf epidermis (on both sides of the leaf) because the water vapor transfer through the leaves varies by potato genotype, where the averaged values of stomatal conductance in the abaxial side could reach almost more than twice the values measured on the adaxial side [88]. Finally, the evaluation of continuously estimated r_c approaches in potato could be an excellent alternative to improve the estimation under different irrigation water levels or combine according to the surface resistance concept that has been done in other crops [43,86,89].

Estimation of ET_{cp} Using LA and LH Approach

The comparison of potato evapotranspiration (ET_{cp}) estimated by soil water balance (ET_{cpWP}) and the Penman–Monteith equation using LA (ET_{cpLA}) and LH (ET_{cpLH}) canopy resistance (r_c) approaches for the full irrigation (IL_1) condition during the 2018/2019 and 2019/2020 seasons are shown in Figure 6. The ET_{cpLA} and ET_{cpLH} overestimated 0.6 and underestimated 11% compared to ET_{cpWP} for both seasons, respectively (Figure 6a,b). Moreover, both estimations presented excellent performance in the statistical evaluation for full irrigation (Table 2). Values of RMSE, MAE, I_a, and t-statistic equal to 4.4 mm, 3.2 mm, 0.8, and 0.1 were reached for ET_{cpLA}, while 4.7 mm, 3.7 mm, 0.7 and 2.6 were observed for ET_{cpLH}, respectively.

Table 2. Statistical evaluation of evapotranspiration over a potato crop estimated by the Penman–Monteith equation using four different canopy resistance models for both seasons (values of Figures 6–8).

ET Models	Irrigation Condition	Total Days (n)	Irrigation Event Ranges (n) [&]	RMSE (mm)	MAE (mm)	I_a	t-Statistic *	r_{eo}	Z-Test
ET_{cpLA}	IL_1	177	26	4.42	3.24	0.82	0.13	1.00	V
ET_{cpLH}	IL_1	177	26	4.75	3.73	0.77	2.66	0.88	F
ET_{cpSL}	IL_1	177	26	5.70	4.63	0.69	4.87	0.78	F
ET_{cpAL}	IL_1	177	26	6.77	5.80	0.60	6.37	0.70	F
ET_{cpLA}	IL_2	177	26	3.24	2.58	0.87	1.72	1.07	V
ET_{cpLH}	IL_2	177	26	3.29	2.69	0.89	2.80	0.89	F
ET_{cpSL}	IL_2	177	26	4.69	3.64	0.74	5.28	0.78	F
ET_{cpAL}	IL_2	177	26	5.71	4.85	0.66	7.66	0.69	F
ET_{cpLA}	IL_3	177	26	8.02	5.94	0.55	1.29	0.87	F
ET_{cpLH}	IL_3	177	26	9.45	6.61	0.52	3.07	0.69	F
ET_{cpSL}	IL_3	177	26	9.62	7.14	0.53	3.72	0.64	F
ET_{cpAL}	IL_3	177	26	11.72	8.58	0.48	4.89	0.48	F

Note: RMSE: root mean square error; MAE: mean absolute error; I_a: index of agreement; r_{eo}: ratio of estimated to observed evapotranspiration values; T: true hypothesis (b = 1); F: false hypothesis (b $\neq$ 1). * The smaller the value of t, the better is the model's performance. IL_1 is a full irrigation, IL_2 is the application of 75% of IL_1, and IL_3 is the application of 60% of IL_1. [&]; total number of irrigation event ranges.

In contrast, in Figure 7, the comparison of ET_{cp} estimated using the LA (ET_{cpLA}) and LH (ET_{cpLH}) r_c approaches and ET_{cpWP} for application of 75% of IL_1 (IL_2) in both seasons are shown. In this case, a lower dispersion of the ET_{cp} values (close to 1:1 line) estimated by ET_{cpLA} and ET_{cpLH} was found. However, there was a higher overestimation of ET_{cp} compared to full irrigation condition for ET_{cpLA} reaching an error close to 7.0%, whereas a similar error was found for ET_{cpLH} (Figure 7a,b). Thus, a RMSE, MAE, I_a, and t-Statistic of 3.2 mm, 2.5 mm, 0.8, and 1.7 for ET_{cpLA} and 3.2 mm, 2.6 mm, 0.8, and 2.8 for ET_{cpLH} was obtained considering both evaluated seasons, respectively (Table 2). Better performance results for some statistical indicators were found for ET_{cpLA} in comparison with ET_{cpLH}

under the IL_3 (application of 60% of IL_1) condition. However, there were higher dispersion values of ET_{cpLA} and ET_{cpLH} compared to the other evaluated irrigation levels, but lower in comparison with the SL (ET_{cpSL}) and AL (ET_{cpLA}) approaches under IL_3 evaluated condition (Table 2).

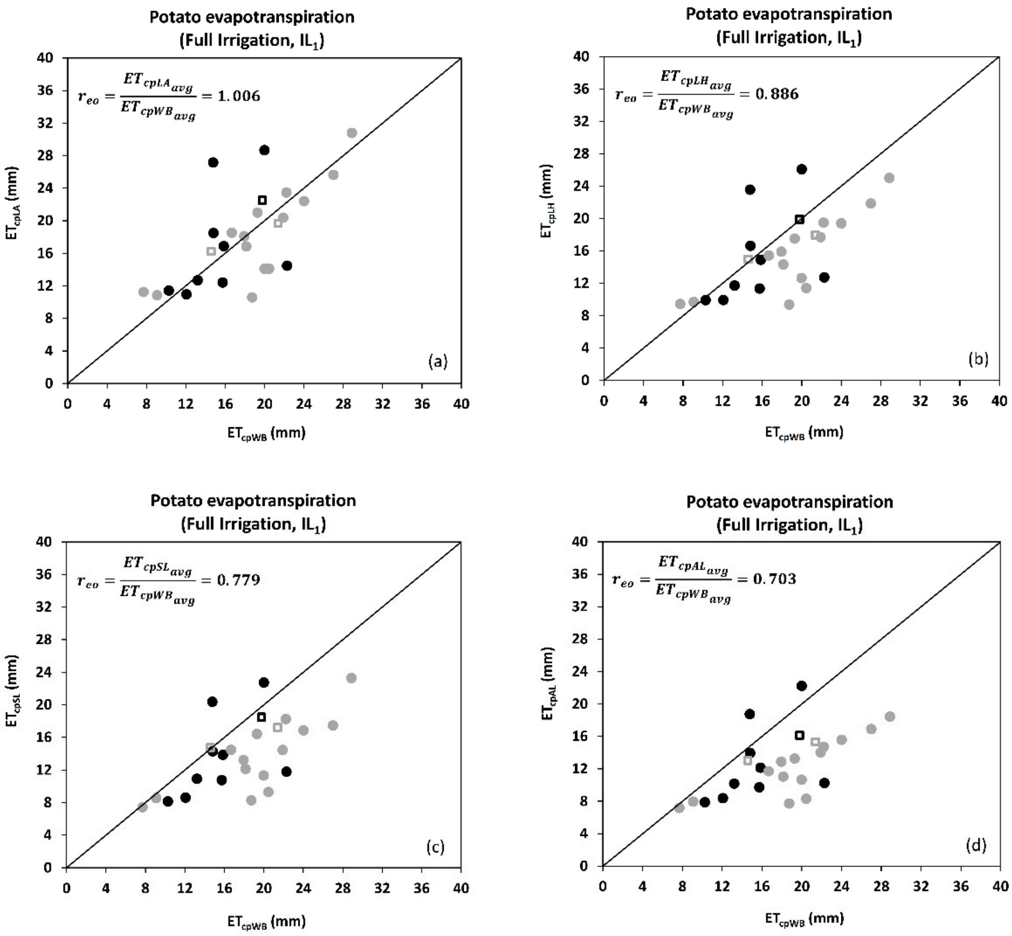

Figure 6. Comparison between potato evapotranspiration estimated by the water balance (ET_{cpWP}) and Penman-Monteith (ET_{cp}) methods using four canopy resistance approaches in full irrigation conditions (IL_1) for both seasons. LA and LH [63], SL [62] and AL [28] corresponding to the canopy resistance (r_c) model at each ET_{cp} approaches used in this study. (**a**), (**b**), (**c**), and (**d**) represent to LA, LH, SL, and AL, rspectively. Closed circles and open squares of black color correspond to the 2018/2019 season, whereas closed circles and open squares of gray color correspond to the 2019/2020 season. Square and circle points represent values of ET when LAI < 2 and LAI > 2, respectively. Each point compares the sum of ET among consecutive irrigation events.

Furthermore, average error values close to 13 and 31% were obtained for ET_{cpLA} and ET_{cpLH}, respectively (Figure 8a,b). Additionally, the frequency distribution of daily range difference between ET_{cpLA} with ET_{cpWP} illustrates that differences greater than ±10 mm were found in less than 4.0% for IL_1, none for IL_2 and 19% for IL_3, while the differences greater than ±10 mm between ET_{cpLH} with ET_{cpWP} were inexistent for IL_1 and IL_2, and 27% for IL_3 (Figure 9a,b,e,f,i,j). On the other hand, the tendency of daily ET_{cpLA} and ET_{cpLH} averages values were similarly observed compared to ET_{cpWP} during the growing and development stages in the three irrigation levels evaluated in both seasons. However, during the 2018/2019 season, heatwave events occurred from 35 (30 DOY) to 41 (36 DOY) and from 43 (38 DOY) to 50 (45 DOY) days after emergence (DAE) during the full flowering period (IF-DF), reaching values of maximum temperature (T_{a_max}) and vapor pressure deficit (VPD) close to 38 °C and 5.0 kPa, respectively (Figure 2).

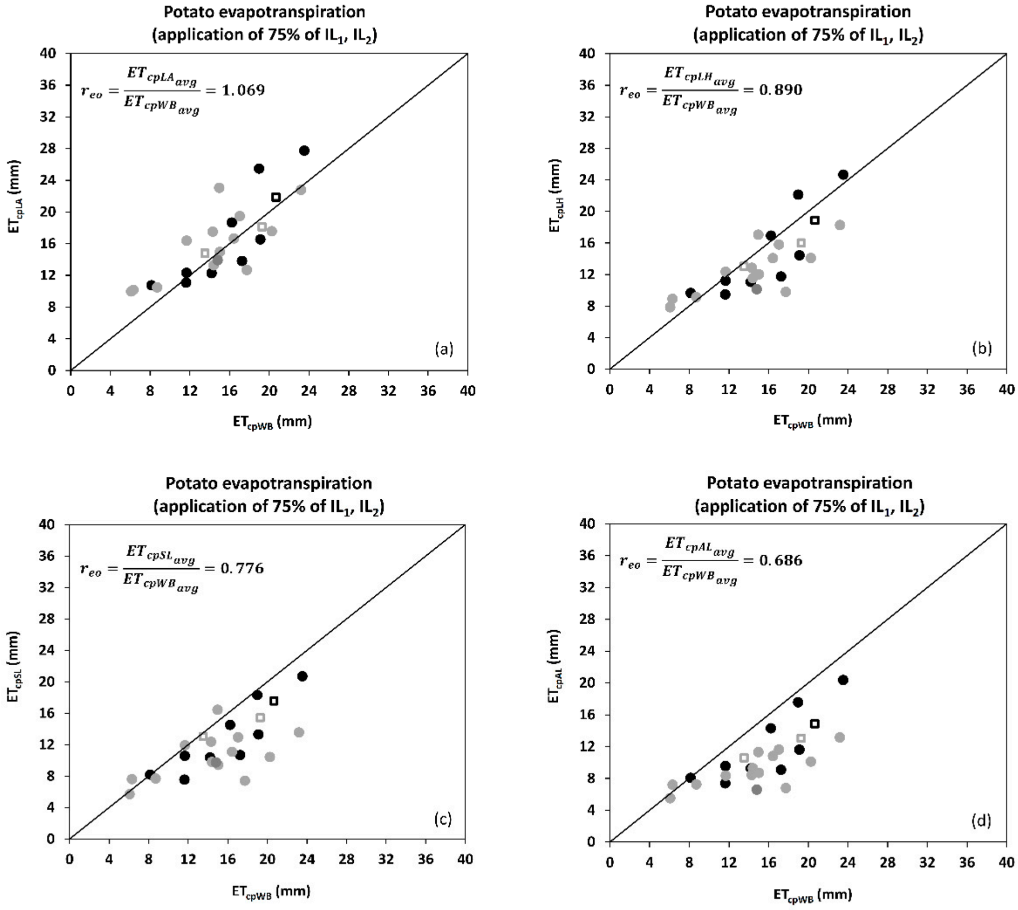

Figure 7. Comparison between potato evapotranspiration estimated by the water balance (ET_{cpWP}) and Penman-Monteith (ET_{cp}) methods using four canopy resistances approaches for the application of 75% of IL_1 (IL_2) in both seasons. LA and LH [63], SL [62] and AL [28] corresponding to the canopy resistance (r_c) model at each ET_{cp} approaches used in this study. (**a**), (**b**), (**c**), and (**d**) represent to LA, LH, SL, and AL, rspectively. Closed circles and open squares of black color correspond to the 2018/2019 season, whereas closed circles and open squares of gray color correspond to the 2019/2020 season. Square and circle points represent values of ET when LAI < 2 and LAI > 2, respectively. Each point compares the sum of ET among consecutive irrigation events.

In almost all cases, an underestimation of ET_{cp} was observed in the evaluated irrigation regimes IL_1 (Figure 10a,c), IL_2 (Figure 11a,c) and IL_3 (Figure 12a,c) with values of 2.0, 4.0 and 4.0% for ET_{cpLA} and 12, 15, and 20% ET_{cpLH} compared to ET_{cpWP}, respectively (Table 3). Likewise, ET_{cpLA} presented a value of RMSE and MAE lower than ET_{cpLH} in all evaluated irrigation levels. For the IL_1 condition, the application of irrigation water did not reach field capacity (FC) during the IE-DF phenological stages (heatwave event), presenting similar values of r_c and LAI than those obtained for IL_2 condition (Figure 5 and Table 1).

Thus, the estimated ET_{cp} was found to underestimate using the LA and LH approaches, and it could be explained by the stomatal regulation of the potato leaves under the different available soil moistures in the rooting zone, and the higher average value of aerodynamic resistance found at noontime (r_a = 30 s m^{-1} between 29–43 DOY and 35–49 DAE), being almost a third of the value found in the same phenological period for IL_1 a condition during the 2019/2020 season (r_a = 22 s m^{-1} between 4–22 DOY or 31–49 DAE). Amer and Hatfield [21] observed a low average value of r_a under available soil water higher than 90% and 2.5 m^2 m^{-2} of LAI at midday conditions in summer. Better performance of ET_{cpLA} and ET_{cpLH} was obtained during the development and maturity periods (finishing the period IE-DF, and between DF-RF and RF-S) for all evaluated irrigation levels, possibly due to the compensation between the low evaporative demand of the atmosphere (Figure 2) and moisture depletion timing of soil (Figure 3b), as r_c was also increased due to leaf senescence typical of the maturity period [21].

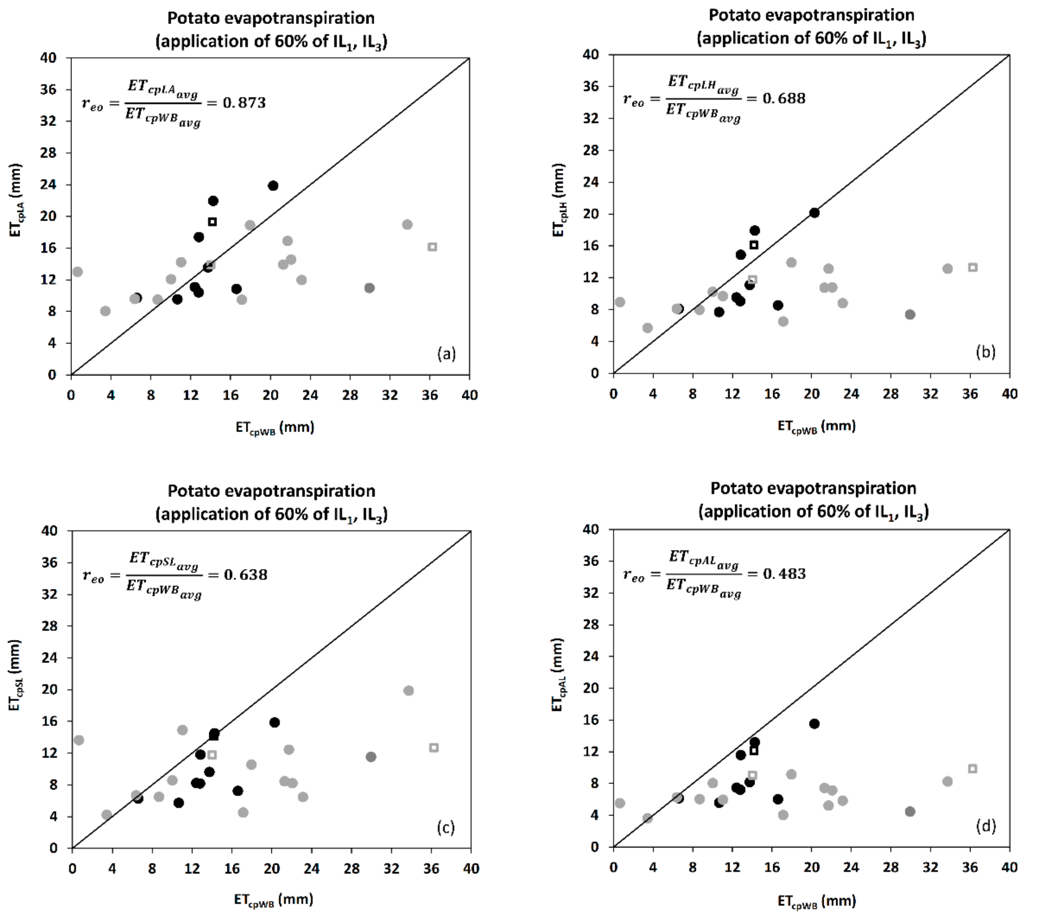

Figure 8. Comparison between potato evapotranspiration estimated by the water balance (ET_{cpWP}) and Penman-Monteith (ET_{cp}) methods using four canopy resistances approaches for the application of 60% of IL_1 (IL_3) in both seasons. LA and LH [63], SL [62] and AL [28] corresponding to the canopy resistance (r_c) model at each ET_{cp} approaches used in this study. (**a**–**d**) represent to LA, LH, SL, and AL, rspectively. Closed circles and open squares of black color correspond to the 2018/2019 season, whereas closed circles and open squares of gray color correspond to the 2019/2020 season. Square and circle points represent values of ET when LAI < 2 and LAI > 2, respectively. Each point compares the sum of ET among consecutive irrigation events.

However, a lower underestimated ET_{cp} was seen during the maximum water demand by the atmosphere for IL_3 condition. It is also necessary to mention that null precipitation was observed in this period, presenting a soil water balance lower than those obtained in the other irrigation levels, being dominated mainly by the depletion of soil moisture present in the effective root zone. Additionally, an increased r_c was observed in comparison with other irrigation conditions but lower than those found by the other evaluated r_c approaches (Figure 5).

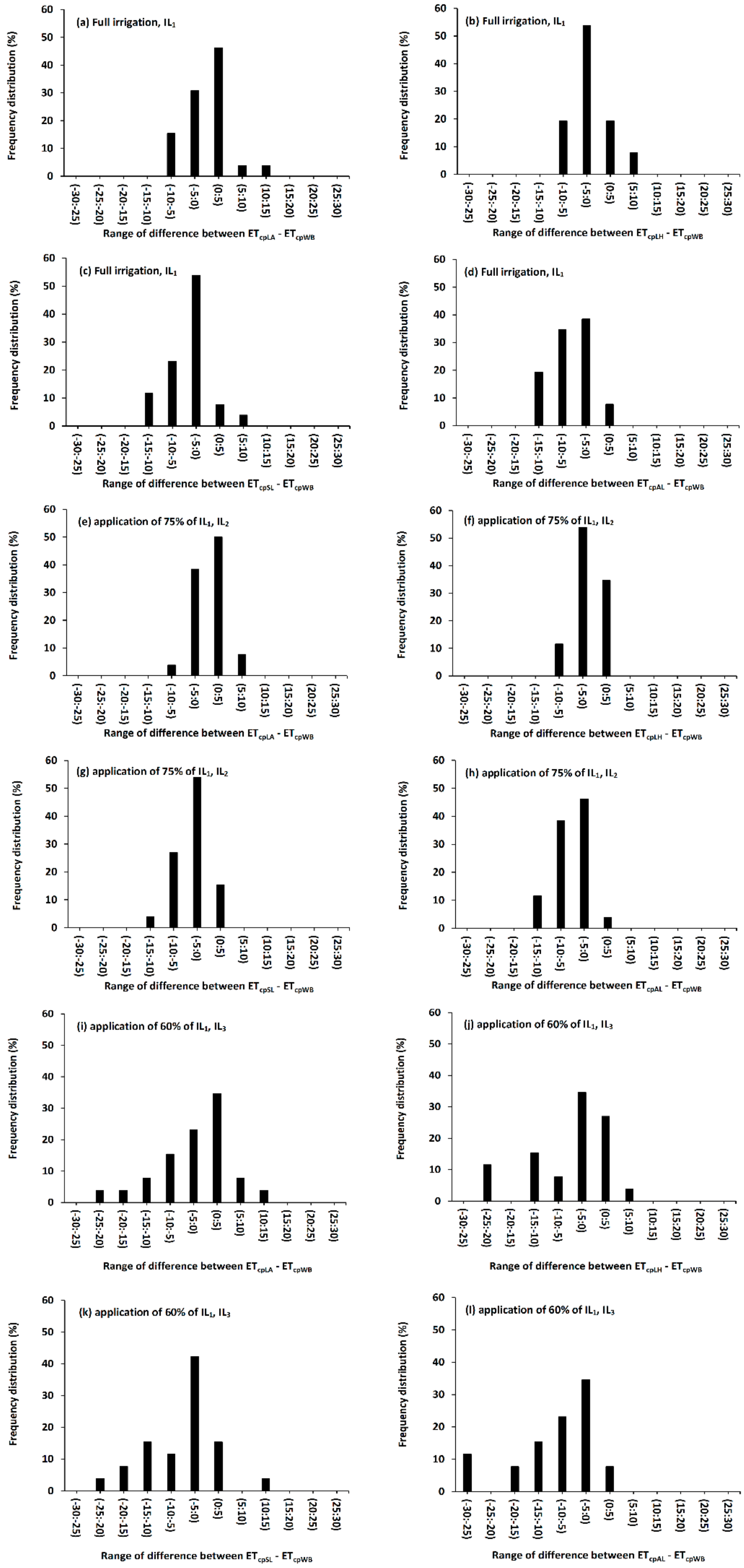

Figure 9. Frequency distribution of daily range difference between ET_{cp} estimated according to the four empirical canopy resistance approaches on a potato crop under IL_1 (**a**–**d**), IL_2 (**e**–**h**) and IL_3 (**i**–**l**) irrigation levels and obtained by soil water balance (ET_{cpWP}) for both evaluated seasons.

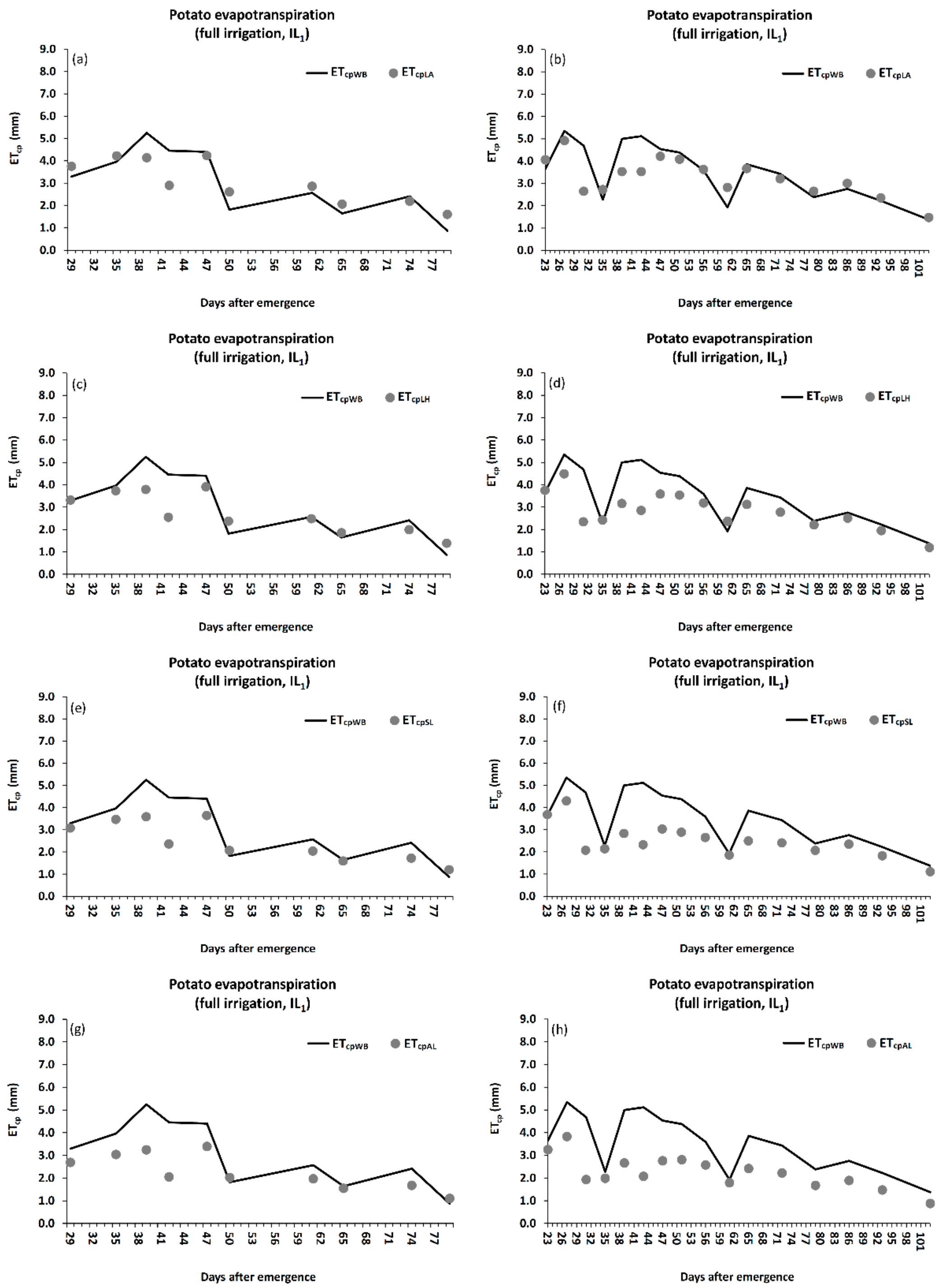

Figure 10. Comparison of daily average ET_{cp} by soil water balance method and PM method with different canopy resistance approaches on a full irrigation condition (IL_1) for 2018/2019 (**a**,**c**,**e**,**g**) and 2019/2020 seasons (**b**,**d**,**f**,**h**).

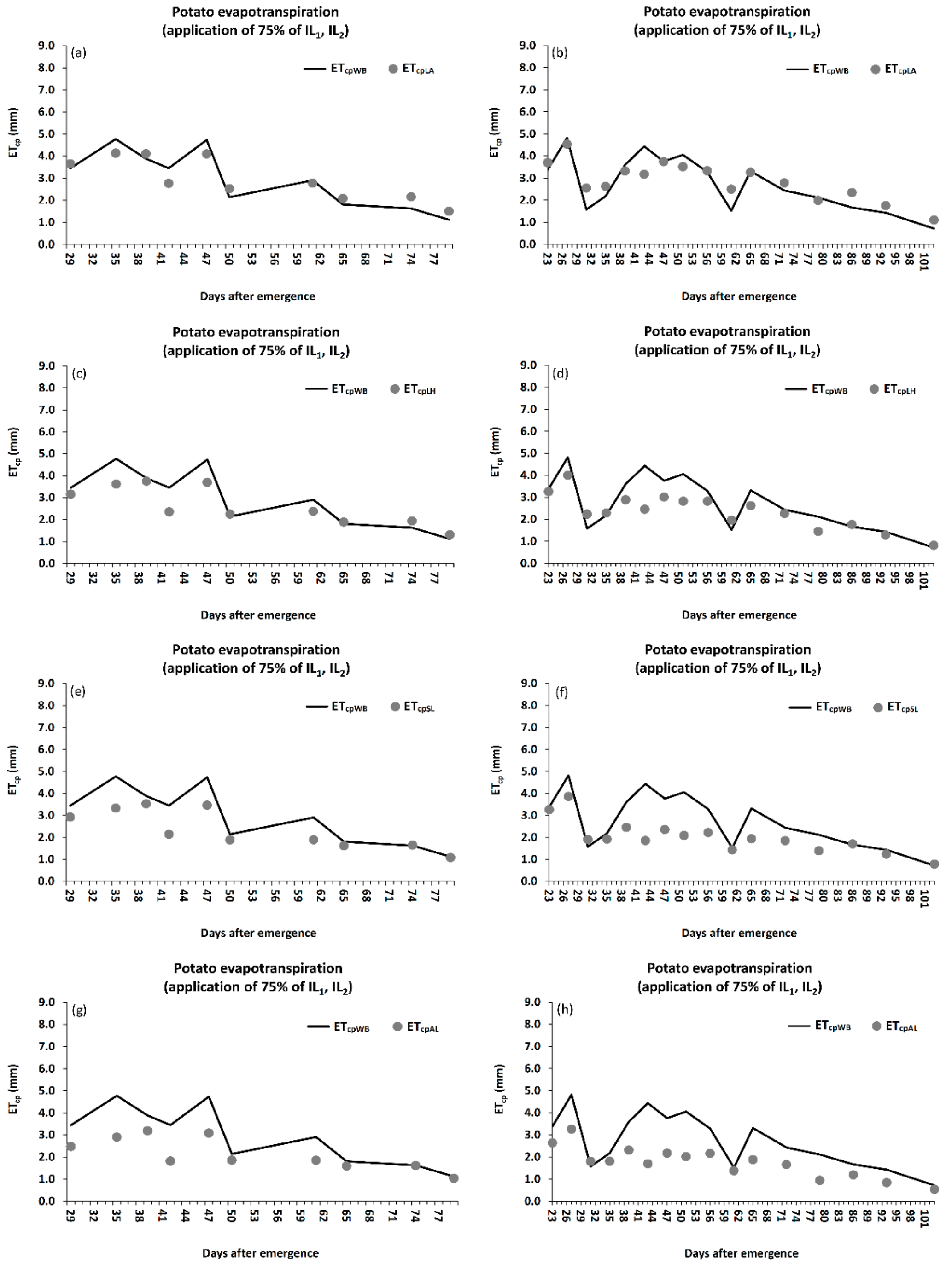

Figure 11. Comparison of daily average ET_{cp} by soil water balance method and PM method with different canopy resistance approaches on an application of 75% of IL_1 (IL_2) for 2018/2019 (**a**,**c**,**e**,**g**) and 2019/2020 seasons (**b**,**d**,**f**,**h**).

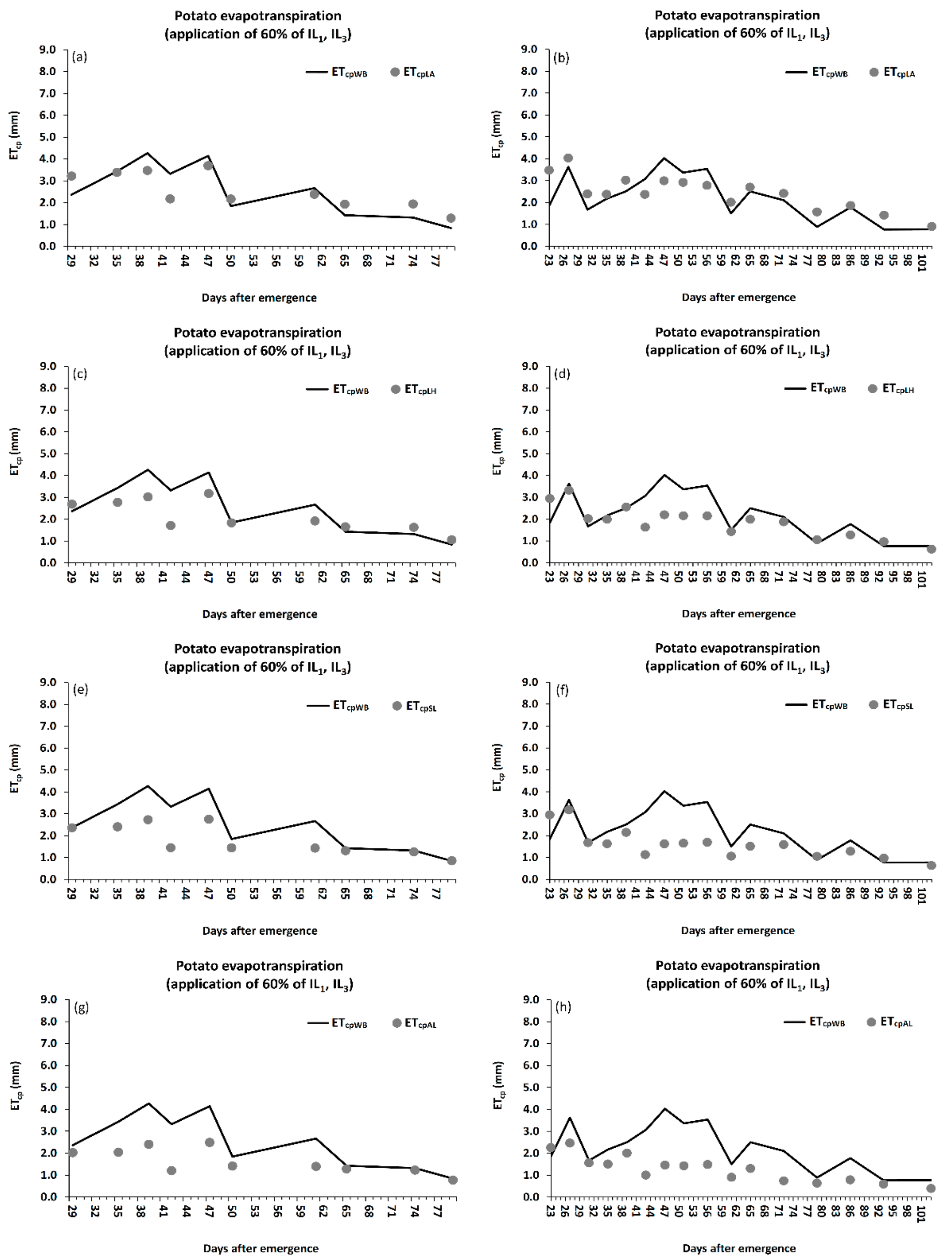

Figure 12. Comparison of daily average ET_{cp} by soil water balance method and PM method with different canopy resistance approaches on an application of 60% of IL_1 (IL_3) for 2018/2019 (**a**,**c**,**e**,**g**) and 2019/2020 seasons (**b**,**d**,**f**,**h**).

During the 2019/2020 season, important heatwave events occurred from 78 (51 DOY) to 80 (53 DOY) and from 87 (60 DOY) to 90 (63 DOY) days after emergence (DAE) during the end of the fruit development (IF-DF) and close to the senescence period (RF-S), reaching values of maximum temperature (T_{a_max}) and vapor pressure deficit (VPD) between 30–33 °C and 2.8–5.1 kPa, respectively (Figure 2). A better estimation of ET_{cp} was seen in the evaluated irrigation regimes IL_1 (Figure 10b,d), where the ET_{cpLA} underestimated 7.0% and the ET_{cpLH} underestimated 20% of ET_{cpWP}, respectively (Table 3), while for IL_2 (Figure 11b,d) and IL_3 (Figure 12b,d), there was an overestimation of less than 9.0%, and an underestimation of less than 16% for ET_{cpLA} and ET_{cpLH} in comparison with ET_{cpWP}, respectively (Table 3). Furthermore, for both ET_{cpLA} and ET_{cpLH}, values of RMSE and MAE less than 1.1 mm d^{-1} were reached for all evaluated irrigation conditions. In this context, a value of RMSE equal to 1.5 mm d^{-1} was obtained by estimating evapotranspiration in maize using the Penman–Monteith model with a coupled surface resistance equation contrasted with the eddy covariance method [44]. Thus, the ET_{cp} was underestimated using the LA and LH approaches almost at the end of the leaf development stage (LD-IE) between 27 (365 DOY) and 31 (4 DOY) days after emergence (DAE) for IL_1. The same tendency was observed at the beginning of flowering (IE-DF) between 39 (12 DOY) and 47 (20 DOY) days after emergence (DAE). However, an improvement of ET_{cp} for IL_1 was observed from 47 to 103 DAE (20–76 DOY) due to the increase in LAI, lower r_c, height crop and the decreasing of the aerodynamic resistance (r_a). In addition, during the developing and maturing (DF to S) phenological stages, a better overlapping of ET_{cp} was observed in both IL_1 and IL_2 condition, because the effect of meteorological variables becomes almost constant (Figure 10b,d). However, for the IL_2 and IL_3 conditions, an underestimated ET_{cp} was seen from 43 to 56 DAE (16–29 DOY). These tendencies could be explained by the lower application of irrigation water (changes in available soil moisture) (Figure 3b), affecting the water transfer from the stomata to the atmosphere by increasing the r_c (Figure 5) [21].

Table 3. Statistical evaluation of daily average ET_{cp} estimated by canopy resistance approach for the different irrigation level conditions on potato crop experiment.

r_c Approaches	Irrigation Condition	2018/2019 Season			2019/2020 Season		
		RMSE (mm d^{-1})	MAE (mm d^{-1})	r_{eo}	RMSE (mm d^{-1})	MAE (mm d^{-1})	r_{eo}
LA	IL_1	0.74	0.60	0.98	0.82	0.57	0.93
LH	IL_1	0.83	0.59	0.88	1.06	0.78	0.80
SL	IL_1	0.95	0.71	0.80	1.35	1.03	0.71
AL	IL_1	1.14	0.88	0.73	1.54	1.27	0.64
LA	IL_2	0.45	0.41	0.96	0.56	0.44	1.04
LH	IL_2	0.65	0.49	0.85	0.75	0.57	0.86
SL	IL_2	0.84	0.64	0.77	1.09	0.81	0.73
AL	IL_2	1.08	0.85	0.69	1.25	1.02	0.64
LA	IL_3	0.63	0.55	0.96	0.68	0.56	1.09
LH	IL_3	0.80	0.63	0.80	0.83	0.61	0.84
SL	IL_3	1.03	0.77	0.68	1.11	0.84	0.71
AL	IL_3	1.21	0.94	0.61	1.27	1.03	0.57

Note: RMSE: root mean square error; MAE: mean absolute error; r_{eo}: ratio of estimated to observed values of evapotranspiration. LA and LH are the r_c model incorporating the concept of amphistomatous and hypostomatous leaves [63], respectively. SL is the r_c model proposed by Szeicz and Long [62]. AL is the more used r_c model proposed by Allen et al. [28]. IL_1 is a full irrigation, IL_2 is the application of 75% of IL_1, and IL_3 is the application of 60% of IL_1.

The ET_{cp} estimation using the different r_c approaches under full irrigation levels presented a reasonable approximation, especially during the advanced stage of the crop (beginning of flowering onwards) (Table 4), not so in early stages (LAI < 1.5 m^2 m^{-2}). According to the results of this study, the use of LA approach (amphistomatous leaves concept) would be the best to estimate ET_{cp} despite the underestimation under conditions of higher water demand by the atmosphere. Preliminary, this calculation method would describe better the relationship between exposed canopy surface and water flow resistance (stomatal resistance) present in both sides of the leaf, in comparison with SL and AL approaches that incorporating a concept associated to that the half of canopy exposition (upper side only) would be active for the vapor transfer [28]. Moreover, the same r_c approach was better observed for estimating ET_{cp} in the different irrigation levels (Table 4), where it could be seen a slight increase in the daily range tendency of ET_{cp} estimated in comparison with the others r_c approaches used. It should be noted that these increased values of ET_{cp} could be associated with the plasticity of the morphological features of potato leaves [77], because it has been observed that stomatal size (SS) and density (SD) could be modulated by environment signal presenting larger SD in a deficit irrigation condition (PRD, Partial root-zone drying) and lower for full irrigation conditions.

Table 4. Evapotranspiration estimated by the canopy resistance approaches, effective rainfall (Ppe, mm) and irrigation (IR, mm) applied in each irrigation level condition during the main potato phenological stages, and maximum water demand by the atmosphere for both seasons.

Phenological Stages	Irrigation Levels	2018/2019 Season							2019/2020 Season						
		ET_{cpWB}	ET_{cpLA}	ET_{cpLH}	ET_{cpSL}	ET_{cpAL}	IR	Ppe	ET_{cpWB}	ET_{cpLA}	ET_{cpLH}	ET_{cpSL}	ET_{cpAL}	IR	Ppe
LD—IE	IL_1	-	-	-	-	-	-	-	38.3 *	41.9 *	38.6 *	37.9 *	33.5 *	79.5	0.0
IE—DF	IL_1	86.9	78.9	70.6	66.1	58.4	103.4	0.0	87.8	71.1	61.5	53.2	49.0	100.4	2.3
DF—RF	IL_1	63.2	70.7	64.3	55.2	53.7	93.1	4.6	96.9	92.1	79.9	65.4	63.6	106.2	14.0
RF—S	IL_1	25.8	30.9	27.2	23.8	22.0	23.7	0.0	59.8	68.7	56.8	53.1	42.7	79.7	0.0
Total	IL_1	175.9	180.5	162.1	145.1	134.1	220.2	4.6	282.8	273.8	236.8	209.6	188.8	365.8	16.3
LD—IE	IL_2	-	-	-	-	-	-	-	28.4 *	37.5 *	32.9 *	32.9 *	26.6 *	59.6	0.0
IE—DF	IL_2	74.5	76.8	67.4	62.5	54.4	77.5	0.0	68.5	66.0	55.3	45.2	42.3	75.0	2.3
DF—RF	IL_2	57.2	70.5	62.6	52.5	51.5	69.8	4.6	70.7	81.7	66.7	50.4	48.9	79.3	14.0
RF—S	IL_2	23.2	28.9	25.2	21.0	20.2	16.1	0.0	73.8	52.3	38.8	37.4	25.6	59.4	0.0
Total	IL_2	154.9	176.2	155.2	136.0	126.1	165.1	4.6	241.4	237.5	193.7	165.9	143.4	273.3	16.3
LD—IE	IL_3	-	-	-	-	-	-	-	38.0 *	33.4 *	27.7 *	27.7 *	20.7 *	47.7	0.0
IE—DF	IL_3	69.7	65.2	54.3	47.4	41.0	62.0	0.0	65.5	56.7	45.1	35.6	32.9	60.0	2.3
DF—RF	IL_3	57.7	62.4	52.3	40.8	39.8	55.9	4.6	60.6	69.1	52.2	40.5	35.4	63.4	14.0
RF—S	IL_3	14.2	25.0	20.6	16.8	15.3	14.2	0.0	50.3	41.4	28.0	28.0	17.1	47.6	0.0
Total	IL_3	141.6	152.6	127.2	105.0	96.1	132.1	4.6	214.4	200.6	153.0	131.8	106.1	218.7	16.3

Note: *: The values presented represent the sum of 40% of the data for the mentioned phenological stage during the 2019/2020 season. LD, IE, DF, RF, and FS are leaf development, inflorescence emergence, development of fruit, ripening of fruit and seed, and finishing of senescence, respectively.

5. Conclusions

This study showed that the highest daytime water vapor resistance activity through the stomata for a potato crop var. Puyehue INIA occurred between 14:00 and 18:00 local time. This result is consistent with all evaluated irrigation levels during both growing seasons. The LA canopy resistance approach provided the best performance for the original Penman–Monteith (P-M) model in the simulation ET_{cp} on a drip-irrigated potato crop. However, significant disagreements of the original P-M model to estimate ET_c directly were associated with arid atmospheric conditions (January–February) occurred mainly during the IF-DF phenological period, independent of the irrigation levels applied and canopy resistance approaches used. Nevertheless, these errors did not considerably affect the overall performance of the original P-M model using mainly the LA and LH canopy resistance approaches for both evaluated seasons. In this context, it is necessary to emphasize that the canopy resistance (r_c) is very variable during daytime and through the potato growing season. Future studies should incorporate other concepts, such as mesophyll conductance and genetic traits, to obtain better performance of ET models under changing conditions. Our analysis showed that it is possible to simulate ET_c on a potato crop considering up to 25% less irrigation water applied at the full irrigation level, using the LA or LH canopy resistance approach combined with the original P-M model. Further studies should be associated with the plasticity of the morphological features of potato leaves and canopy geometry, as the stomatal water vapor flowing on the canopy surface could be affected, a key factor in the canopy resistance concept for accurate ET estimation under soil-water-limited conditions.

Author Contributions: Conceptualization, R.L.-O.; methodology, R.L.-O., S.F. and C.P.-E.; software, R.L.-O.; validation, R.L.-O., S.F., C.P.-E. and V.Q.-A.; formal analysis, R.L.-O., S.F. and C.P.-E.; investigation, resources, R.L.-O.; data creation, R.L.-O., V.Q.-A. and L.M.; writing—original draft preparation, R.L.-O. and S.F.; writing—review and editing, R.L.-O., S.F. and C.P.-E.; visualization, R.L.-O., S.F. and C.P.-E.; supervision, R.L.-O.; project administration, R.L.-O.; funding acquisition, R.L.-O. All authors have read and agreed to the published version of the manuscript.

Funding: This research and publication were supported by the Chilean government through the Agencia Nacional de Investigación y Desarrollo (ANID) throughout the "Programa FONDECYT Iniciación en la Investigación, año 2018" (grant No. 11180667).

Institutional Review Board Statement: Not applicable.

Informed Consent Statement: Not applicable.

Data Availability Statement: Data acquired from this research are proprietary to INIA as intellectual property, and sharing needs to be discussed on a case-by-case basis and under collaboration agreements between INIA and a third party.

Acknowledgments: We would like to thank the field and technical support team of irrigation science of INIA Carillanca (Edgardo Estrada, Rafael Castro, Pedro Bustos, Rubén Velazquez). The authors acknowledge the contribution of Claudia Gonzalez Viejo from the University of Melbourne for her help informating and processing the paper.

Conflicts of Interest: The authors declare no conflict of interest.

References

1. FAO. *World Food and Agriculture—Statistical Yearbook 2021*; FAO: Rome, Italy, 2021. [CrossRef]
2. Bártová, V.; Bárta, J.; Brabcová, A.; Zdráhal, Z.; Horáčková, V. Amino acid composition and nutritional value of four cultivated South American potato species. *J. Food Compos. Anal.* **2015**, *40*, 78–85. [CrossRef]
3. Devaux, A.; Kromann, P.; Ortiz, O. Potatoes for Sustainable Global Food Security. *Potato Res.* **2014**, *57*, 185–199. [CrossRef]
4. INE. Statistical Database of Agricultural, Forest and Livestock 2021. Available online: https://www.ine.cl/estadisticas/economia/agricultura-agroindustria-y-pesca (accessed on 25 May 2022).
5. Valdés-Pineda, R.; Pizarro, R.; García-Chevesich, P.; Valdés, J.B.; Olivares, C.; Vera, M.; Balocchi, F.; Pérez, F.; Vallejos, C.; Fuentes, R.; et al. Water governance in Chile: Availability, management and climate change. *J. Hydrol.* **2014**, *519*, 2538–2567. [CrossRef]
6. López-Olivari, R. *Manejo y Uso Eficiente del Agua de Riego Intrapredial Para el Sur de Chile: Conceptos y Consideraciones Básicas en Métodos y Programación de Riego para Optimizar el Recurso Hídrico*, 1st ed.; Instituto de Investigaciones Agropecuarias (INIA-Chile), Centro Regional Carillanca-Temuco: Temuco, Chile, 2016; pp. 6–10.
7. Liu, F.; Shahnazari, A.; Andersen, M.N.; Jacobsen, S.-E.; Jensen, C.R. Physiological responses of potato (*Solanum tuberosum* L.) to partial root-zone drying: ABA signalling, leaf gas exchange, and water use efficiency. *J. Exp. Bot.* **2006**, *57*, 3727–3735. [CrossRef]
8. El Bergui, O.; Abouabdillah, A.; Bouabid, R.; El Jaouhari, N.; Brouziyne, Y.; Bourioug, M. Agro-physiological response of potato to "sustainable" deficit irrigation in the plain of Saïs, Morocco. *E3S Web Conf.* **2020**, *183*, 03001. [CrossRef]
9. Chai, Q.; Gan, Y.; Zhao, C.; Xu, H.-L.; Waskom, R.M.; Niu, Y.; Siddique, K.H.M. Regulated deficit irrigation for crop production under drought stress. A review. *Agron. Sustain. Dev.* **2016**, *36*, 1–21. [CrossRef]
10. Yactayo, Y.; Ramírez, D.A.; Gutiérrez, R.; Mares, V.; Posadas, A.; Quiroz, R. Effect of partial root-zone drying irrigation timing on potato tuber yield and water use efficiency. *Agric. Water Manag.* **2013**, *123*, 65–70. [CrossRef]
11. Yuan, B.-Z.; Nishiyama, S.; Kang, Y. Effects of different irrigation regimes on the growth and yield of drip-irrigated potato. *Agric. Water Manag.* **2003**, *63*, 153–167. [CrossRef]
12. Onder, S.; Caliskan, M.E.; Onder, D.; Caliskan, S. Different irrigation methods and water stress effects on potato yield and yield components. *Agric. Water Manag.* **2005**, *73*, 73–86. [CrossRef]
13. Shahnazari, A.; Liu, F.; Andersen, M.N.; Jacobsen, S.-E.; Jensen, C.R. Effects of partial root-zone drying on yield, tuber size and water use efficiency in potato under field conditions. *Field Crops Res.* **2007**, *100*, 117–124. [CrossRef]
14. Ierna, A.; Mauromicale, G. Tuber yield and irrigation water productivity in early potatoes as affected by irrigation regime. *Agric. Water Manag.* **2012**, *115*, 276–284. [CrossRef]
15. Alva, A.K.; Moore, A.D.; Collins, H.P. Impact of Deficit Irrigation on Tuber Yield and Quality of Potato Cultivars. *J. Crop Improv.* **2012**, *26*, 211–227. [CrossRef]
16. Ahmadi, S.H.; Agharezaee, M.; Kamgar-Haghighi, A.A.; Sepaskhah, A.R. Effects of dynamic and static deficit and partial root zone drying irrigation strategies on yield, tuber sizes distribution, and water productivity of two field grown potato cultivars. *Agric. Water Manag.* **2014**, *134*, 126–136. [CrossRef]
17. Carli, C.; Yuldashev, F.; Khalikov, D.; Condori, B.; Mares, V.; Monneveux, P. Effect of different irrigation regimes on yield, water use efficiency and quality of potato (*Solanum tuberosum* L.) in the lowlands of Tashkent, Uzbekistan: A field and modeling perspective. *Field Crops Res.* **2014**, *163*, 90–99. [CrossRef]
18. Gordon, R.; Brown, D.M.; Madani, A.; Dixon, M.A. An assessment of potato sap flow as affected by soil water status, solar radiation and vapour pressure deficit. *Can. J. Soil Sci.* **1999**, *79*, 245–253. [CrossRef]
19. Rana, G.; Katerji, N. Measurement and estimation of actual evapotranspiration in the field under Mediterranean climate: A review. *Eur. J. Agron.* **2000**, *13*, 125–153. [CrossRef]

20. Zhang, L.; Dawes, W.R.; Walker, G.R. Response of mean annual evapotranspiration to vegetation changes at catchment scale. *Water Resour. Res.* **2001**, *37*, 701–708. [CrossRef]
21. Amer, K.H.; Hatfield, J.L. Canopy Resistance as Affected by Soil and Meteorological Factors in Potato. *Agron. J.* **2004**, *96*, 978–985. [CrossRef]
22. Farahani, H.J.; Howell, T.A.; Shuttleworth, W.J.; Bausch, W.C. Evapotranspiration: Progress in measurement and modeling in agriculture. *Trans. ASABE* **2007**, *50*, 1627–1638. [CrossRef]
23. Jung, M.; Reichstein, M.; Ciais, P.; Seneviratne, S.I.; Sheffield, J.; Goulden, M.L.; Bonan, G.; Cescatti, A.; Chen, J.; De Jeu, R.; et al. Recent decline in the global land evapotranspiration trend due to limited moisture supply. *Nature* **2010**, *467*, 951–954. [CrossRef]
24. Bastiaanssen, W.G.M.; Cheema, M.J.M.; Immerzeel, W.W.; Miltenburg, I.J.; Pelgrum, H. Surface energy balance and actual evapotranspiration of the transboundary Indus Basin estimated from satellite measurements and the ETLook model. *Water Resour. Res.* **2012**, *48*, 1–16. [CrossRef]
25. Li, S.; Kang, S.; Zhang, L.; Li, F.; Hao, X.; Ortega-Farias, S.; Guo, W.; Ji, S.; Wang, J.; Jiang, X. Quantifying the combined effects of climatic, crop and soil factors on surface resistance in a maize field. *J. Hydrol.* **2013**, *489*, 124–134. [CrossRef]
26. Petropoulos, G.P.; Srivastava, P.K.; Piles, M.; Pearson, S. Earth Observation-Based Operational Estimation of Soil Moisture and Evapotranspiration for Agricultural Crops in Support of Sustainable Water Management. *Sustainability* **2018**, *10*, 181. [CrossRef]
27. Ma, N.; Szilagyi, J.; Zhang, Y. Calibration-Free Complementary Relationship Estimates Terrestrial Evapotranspiration Globally. *Water Resour. Res.* **2021**, *57*, e2021WR029691. [CrossRef]
28. Allen, R.; Pereira, L.; Smith, M. *Crop Evapotranspiration-Guidelines for Computing Crop Water Requirements-FAO Irrigation and Drainage*; FAO: Rome, Italy, 1998; Volume 56.
29. Kashyap, P.S.; Panda, R.K. Evaluation of evapotranspiration estimation methods and development of crop-coefficients for potato crop in a sub-humid region. *Agric. Water Manag.* **2001**, *50*, 9–25. [CrossRef]
30. Kadam, S.A.; Gorantiwar, S.D.; Mandre, N.P.; Tale, D.P. Crop Coefficient for Potato Crop Evapotranspiration Estimation by Field Water Balance Method in Semi-Arid Region, Maharashtra, India. *Potato Res.* **2021**, *64*, 421–433. [CrossRef]
31. Ortega-Farias, S.; Irmak, S.; Cuenca, R.H. Editorial: Special issue on evapotranspiration measurement and modeling. *Irrig. Sci.* **2009**, *28*, 1–3. [CrossRef]
32. Ortega-Farias, S.; Olioso, A.; Antonioletti, R.; Brisson, N. Evaluation of the Penman-Monteith model for estimating soybean evapotranspiration. *Irrig. Sci.* **2004**, *23*, 1–9. [CrossRef]
33. Jarvis, P.G. The interpretation of the variations in leaf water potential and stomatal conductance found in canopies in the field. *Philos. Trans. R. Soc. B Biol. Sci.* **1976**, *273*, 593–610. [CrossRef]
34. Katerji, N.; Perrier, A. Modélisation de l'évapotranspiration réelle d'uneparcelle de luzerne: Rôle d'un coefficient cultural. *Agronomie* **1983**, *3*, 513–521. [CrossRef]
35. Stewart, J.B. Modeling surface conductance of pine forest. *Agric. For. Meteorol.* **1988**, *43*, 19–35. [CrossRef]
36. Shuttleworth, W.J.; Gurney, R.J. The theoretical relationship between foliage temperature and canopy resistance in sparse crops. *Q. J. R. Meteorol. Soc.* **1990**, *116*, 497–519. [CrossRef]
37. Massman, W.J. A surface energy balance method for partitioning evapotranspiration data into plant and soil components for a surface with partial canopy cover. *Water Resour. Res.* **1992**, *28*, 1723–1732. [CrossRef]
38. Stannard, D.I. Comparison of Penman–Monteith, Shuttleworth-Wallace, and modified Priestley–Taylor evapotranspiration models for wildland vegetation in semiarid rangeland. *Water Resour. Res.* **1993**, *29*, 1379–1392. [CrossRef]
39. Todorovic, M. Single-layer evapotranspiration model with variable canopy resistance. *J. Irrig. Drain.* **1999**, *125*, 35–245. [CrossRef]
40. Leuning, R.; Zhang, Y.Q.; Rajaud, A.; Cleugh, H.; Tu, K. A simple surface conductance model to estimate regional evaporation using MODIS leaf area index and the Penman–Monteith equation. *Water Resour. Res.* **2008**, *44*, W10419. [CrossRef]
41. García-Santos, G.; Bruijnzeel, L.A.; Dolman, A.J. Modelling canopy conductance under wet and dry conditions in a subtropical cloud forest. *Agric. For. Meteorol.* **2009**, *149*, 1565–1572. [CrossRef]
42. Irmak, S.; Mutiibwa, D. On the dynamics of canopy resistance: Generalized linear estimation and relationships with primary micrometeorological variables. *Water Resour. Res.* **2010**, *46*, W08526. [CrossRef]
43. Li, S.; Zhang, L.; Kang, S.; Tong, L.; Du, T.; Hao, X.; Zhao, P. Comparison of several surface resistance models for estimating crop evapotranspiration over the entire growing season in arid regions. *Agric. For. Meteorol.* **2015**, *208*, 1–15. [CrossRef]
44. Li, S.; Hao, X.; Du, T.; Tong, L.; Zhang, J.; Kang, S. A coupled surface resistance model to estimate crop evapotranspiration in arid region of northwest China. *Hydrol. Process.* **2014**, *28*, 2312–2323. [CrossRef]
45. Kalazich, J.; Uribe, M.; Santos, J.; López, H.; Acuña, I.; Orena, S.; Catalán, P.; Winkler, A. *Puyehue-INIA: Variedad de Papa de Alto Rendimiento, Piel Roja, Pulpa Amarilla y Gran Calidad Para Consumo Fresco*; Informativo INIA Remehue: Osorno, Chile, 2013; No. 111.
46. López-Olivari, R.; Ortega-Klose, F. Response of red clover to deficit irrigation: Dry matter yield, populations, and irrigation water use efficiency in southern Chile. *Irrig. Sci.* **2021**, *39*, 173–189. [CrossRef]
47. *CIREN Descripciones de Suelos, Materiales y Símbolos. Estudio Agrológico IX Región*; Publicación N° 122; Centro de Información de Recursos Naturales (CIREN): Santiago, Chile, 2002; 360p.
48. Suleiman, A.A.; Tojo Soler, C.M.; Hoogenboom, J. Evaluation of FAO-56 crop coefficient procedures for deficit irrigation management of cotton in a humid climate. *Agric. Water Manag.* **2007**, *91*, 33–42. [CrossRef]

49. Fouli, Y.; Duiker, S.W.; Fritton, D.D.; Hall, M.H.; Watsond, J.E.; Johnsone, D.H. Double cropping effects on forage yield and the field water balance. *Agric. Water Manag.* **2012**, *115*, 104–117. [CrossRef]
50. Taghvaeian, S.; Chávez, J.L.; Bausch, W.C.; DeJonge, K.C.; Trout, T.J. Minimizing instrumentation requirement for estimating crop water stress index and transpiration of maize. *Irrig. Sci.* **2014**, *32*, 53–65. [CrossRef]
51. Schneider, C.; Rasband, W.; Eliceiri, K. NIH Image to ImageJ: 25 years of image analysis. *Nat. Methods* **2012**, *9*, 671–675. [CrossRef]
52. Rolando, J.L.; Ramírez, D.A.; Yactayo, W.; Monneveux, P.; Quiroz, R. Leaf greenness as a drought tolerance related trait in potato (*Solanum tuberosum* L.). *Environ. Exp. Bot.* **2015**, *110*, 27–35. [CrossRef]
53. Hack, H.; Gall, H.; Klemke, T.; Klose, R.; Meier, U.; Stauss, R.; Witzenberger, A. Phänologische Entwicklungsstadien der Kartoffel (*Solanum tuberosum* L.). Codierung und Beschreibung nach der erweiterten BBCH-Skala mit Abbildungen. *Nachrichtenbl. Deut. Pflanzenschutzd.* **1993**, *45*, 11–19.
54. Poblete-Echeverría, C.; Ortega-Farias, S. Estimation of actual evapotranspiration for a drip-irrigated Merlot vineyard using a three-source model. *Irrig. Sci.* **2009**, *28*, 65–78. [CrossRef]
55. Agam, N.; Kustas, W.P.; Alfieri, J.G.; Gao, F.; McKee, L.M.; Prueger, J.H.; Hipps, L.E. Micro-scale spatial variability in soil heat flux (SHF) in a wine-grape vineyard. *Irrig. Sci.* **2019**, *37*, 253–268. [CrossRef]
56. Higashi, A. On the Thermal Conductivity of Soil. *J. Fac. Sci. Hokkaido Univ. Ser. 2* **1951**, *4*, 21–29.
57. Kasubuchi, T. Twin isothermal calorimeter method for the determination of specific heat of soil. *Soil Sci. Plant Nutr.* **1975**, *21*, 73–77. [CrossRef]
58. Maeda, T.; Takenaka, H.; Warkentin, B.P. Physical Properties of Allophane Soils. *Adv. Agron.* **1977**, *29*, 229–264. [CrossRef]
59. Mayer, D.G.; Butler, D.G. Statistical validation. *Ecol. Model.* **1993**, *68*, 21–31. [CrossRef]
60. Stone, R.J. Improved statistical procedure for the evaluation of solar radiation estimation models. *Sol. Energy* **1993**, *51*, 289–291. [CrossRef]
61. Willmott, C.J. On the validation of models. *Phys. Geogr.* **1981**, *2*, 184–194. [CrossRef]
62. Szeicz, G.; Long, I.F. Surface resistance of crop canopies. *Water Resour. Res.* **1969**, *5*, 622–633. [CrossRef]
63. Lhomme, J.P.; Montes, C.; Jacob, F.; Prévot, L. Evaporation from Heterogeneous and Sparse Canopies: On the Formulations Related to Multi-Source Representations. *Bound-Lay Meteorol.* **2012**, *144*, 243–262. [CrossRef]
64. Tech, C. *Introduction to Mathematical Modeling of Crop Growth: How the Equations are Derived and Assembled into a Computer Program*; Brown Walker Press: Boca Raton, FL, USA, 2006; 256p.
65. Pachepsky, L.R.; Muschak, M.; Acock, R.; Kobmann, J.; Blechschmidt-Schneider, S.; Willmitzer, L.; Fisahn, J. Calculating leaf boundary layer parameters with the two-dimensional model 2DLEAF comparing transpiration rates of normal (cv. Desiree) and transgenic (sucrose transport antisense) potato plants. *Biotronics* **1998**, *27*, 41–52.
66. Wang, Q.; Fleisher, D.H.; Timlin, D.; Reddy, V.R.; Chun, J.A. Quantifying the measurement errors in a portable open gas-exchange system and their effects on the parameterization of Farquhar et al. model for C3 leaves. *Photosynthetica* **2012**, *50*, 223–238. [CrossRef]
67. Miskoska-Milevska, E.; Dimovska, D.; Popovski, Z.T.; Iljovski, I. Influence of the fertilizers Slavol and Biohumus on potato leaf area and stomatal density. *Acta Agric. Serbica* **2020**, *25*, 13–17. [CrossRef]
68. Katerji, N.; Rana, G. Modelling evapotranspiration of six irrigated crops under Mediterranean climate conditions. *Agric. For. Meteorol.* **2006**, *138*, 142–155. [CrossRef]
69. Pereira, L.S.; Alves, I. Crop water requirements. In *Encyclopedia of Soils in the Environment*, 1st ed.; Hillel, D., Ed.; Elsevier: London, UK; New York, NY, USA, 2005; pp. 322–334. [CrossRef]
70. Vachaud, G.; Vauclin, M.; Riou, C.; Chaabouni, Z. Evapotranspiration en zone semi-aride de deux couverts veÂgeÂtaux (gazon, bleÂ) obtenue par plusieurs meÂthodes II. MeÂthodes neutroniques et tensiomeÂtriques. *Agronomie* **1985**, *5*, 267–274. [CrossRef]
71. Franco, J.A.; Abrisqueta, J.M.; Hernansáez, A.; Moreno, F. Water balance in a young almond orchard under drip irrigation with water of low quality. *Agric. Water Manag.* **2000**, *43*, 75–98. [CrossRef]
72. Wang, F.-X.; Kang, Y.; Liu, S.-P. Effects of drip irrigation frequency on soil wetting pattern and potato growth in North China Plain. *Agric. Water Manag.* **2006**, *79*, 248–264. [CrossRef]
73. Harms, T.E.; Konschuh, M.N. Water savings in irrigated potato production by varying hill–furrow or bed–furrow configuration. *Agric. Water Manag.* **2010**, *97*, 1399–1404. [CrossRef]
74. Wen, A.; Zhang, H.; Zhang, J. Photosynthetic Physiology Characteristics of Potato (*Solanum Tuberosum*) at Tuber Initiation Responses to Water Deficit Regulated with Mulched Drip Irrigation. *Adv. Mat. Res.* **2014**, *838–841*, 2370–2373. [CrossRef]
75. Wheeler, R.M.; Fitzpatrick, A.H.; Tibbitts, T.W. Potatoes as a Crop for Space Life Support: Effect of CO_2, Irradiance, and Photoperiod on Leaf Photosynthesis and Stomatal Conductance. *Front. Plant Sci.* **2019**, *10*, 1632. [CrossRef]
76. Hill, D.; Nelson, D.; Hammond, J.; Bell, L. Morphophysiology of Potato (*Solanum tuberosum*) in Response to Drought Stress: Paving the Way Forward. *Front. Plant Sci.* **2021**, *11*, 597554. [CrossRef]
77. Sun, Y.; Yan, F.; Cui, X.; Liu, F. Plasticity in stomatal size and density of potato leaves under different irrigation and phosphorus regimes. *J. Plant Physiol.* **2014**, *171*, 1248–1255. [CrossRef]
78. Sam, O.; Jeréz, E.; García, D.; Estévez, A.; Falcón, V.; de la Rosa, M.C. Anatomical characteristics of the leaf epidermis of potato plants (*Solanum tuberosum* L.) under water deficit conditions. *Rev. Cultiv. Trop.* **1997**, *18*, 31–37.
79. Kjelgaard, J.F.; Stockle, C.O. Evaluating surface resistance for estimating corn and potato evapotranspiration with the Penman-Monteith model. *Trans. ASAE* **2001**, *44*, 797–805. [CrossRef]

80. Monteith, J.L. Accomodation between transpiring vegetation and the convective boundary layer. *J. Hydrol.* **1995**, *166*, 251–263. [CrossRef]
81. Alves, I.; Pereira, L.S. Modeling surface resistance from climatic variables? *Agric. Water Manag.* **2000**, *42*, 371–385. [CrossRef]
82. Lecina, S.; Martinez-Cob, A.; Ṕerez, P.G.; Villalobos, F.J.; Baselga, J.J. Fixed versus bulk canopy resistance for reference evapotranspiration estimation using the Penman–Monteith equation under semiarid conditions. *Agric. Water Manag.* **2003**, *60*, 181–198. [CrossRef]
83. Gharsallah, O.; Facchi, A.; Gandolfi, C. Comparison of six evapotranspiration models for a surface irrigated maize agro-ecosystem in Northern Italy. *Agric. Water Manag.* **2013**, *130*, 119–130. [CrossRef]
84. Srivastava, R.K.; Panda, R.K.; Chakraborty, A.; Halder, D. Comparison of actual evapotranspiration of irrigated maize in a sub-humid region using four different canopy resistance based approaches. *Agric. Water Manag.* **2018**, *202*, 156–165. [CrossRef]
85. Hatfield, J.L. Wheat canopy resistance determined by energy balance techniques. *Agron. J.* **1985**, *77*, 279–283. [CrossRef]
86. Rana, G.; Katerji, N.; Mastrorilli, M. Canopy resistance modelling for crops in contrasting water conditions. *Phys. Chem. Earth* **1998**, *23*, 433–438. [CrossRef]
87. Katerji, N.; Rana, G.; Fahed, S. Parameterizing canopy resistance using mechanistic and semi-empirical estimates of hourly evapotranspiration: Critical evaluation for irrigated crops in the Mediterranean. *Hydrol. Process* **2011**, *25*, 117–129. [CrossRef]
88. Bhagsari, A.S.; Webb, R.E.; Phatak, S.C.; Jaworski, C.A. Canopy photosynthesis, stomatal conductance and yield of Solanum tuberosum grown in a warm climate. *Am. Potato J.* **1988**, *65*, 393–406. [CrossRef]
89. Rana, G.; Katerji, N.; Mastorilli, M.; El Moujabber, M. A model for predicting actual evapotranspiration under water stress conditions in a Mediterranean region. *Theor. Appl. Climatol.* **1997**, *56*, 45–55. [CrossRef]